INVESTIGATING THE IMPACT OF HIV INFECTION ON ILC3S IN HUMAN LYMPH NODES

Nicholas Graeme Herbert

Submitted in fulfilment of the requirements for the degree of Master of Medical Sciences in the School of Virology, University of KwaZulu-Natal.

May 2022

Mr. Nicholas Herbert

[redacted]

Dr. Henrik Kløverpris

[redacted]

DECLARATION

I, Nicholas Graeme Herbert, declare as follows:

1. That the work described in this thesis has not been submitted to UKZN or other tertiary institution for purposes of obtaining an academic qualification, whether by myself or any other party.

2. That my contribution to the project was as follows:

   I was involved in selecting what lymph node scRNA-seq samples and formalin-fixed paraffin-embedded tissue (FFPE) samples were used in this dissertation. I converted the single cell RNA-seq (scRNA-seq) data from Bcl2 files to FASTQ files, and thereafter trimmed and aligned the FASTQ files, all using Terra Workspace. I did all initial quality control processing of the scRNA-seq data using Seurat Package on RStudio. I analysed and produced all the scRNA-seq data that appears in the manuscript. I also processed most of the FFPE lymph nodes and did quality checks (H&E stains) and subsequent immunohistochemistry experiments. I also acquired all the immunohistochemistry images that appear in the manuscript, as well as previous optimization experiments. I, along with the guidance of Dr. Henrik Kløverpris, conceived the aim and hypotheses for this project.

3. That the contributions of others to the project were as follows:

   Emmanuel Asowata and Yenzekile Zungu (previous members of the Kløverpris Lab), conducted the tissue processing, cell sorting and subsequent Seq-Well experiments. Rabiah Fardoos (previous member of the Kløverpris Lab) conducted the sequencing of the samples at the University of Copenhagen. Some fresh lymph nodes were processed by Emmanuel Asowata into FFPE tissue. Dr. Henrik Kløverpris established the 'Gut Associated Lymphoid Tissue' cohort.

4. Signed ___ 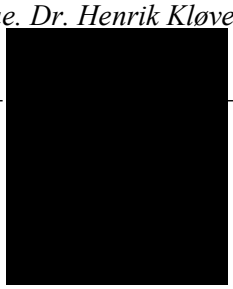 ____ Date: 30/05/22

ACKNOWLEDGEMENTS

I would like to acknowledge:

Dr. Emmanuel Asowata for training me on fluorescent immunohistochemistry and for giving me invaluable advise when I first arrived at the Africa Health Research Institute. Your guidance gave me confidence and allowed me to find my feet when I first started.

Dr. Ian Mbano for helping me initially with processing single cell RNA-seq data. To Prof. Alex K. Shalek and Connor Kummerlowe for assisting me with the FASTQ file processing and for inviting me to join them at the Broad Institute, although the COVID-19 pandemic/PhD opportunity prevented me from going. To Sarah Nyquist and Connor Kummerlowe for assisting me with the various functions in Seurat package, which helped me immensely.

The members of the Leslie Lab and the Kløverpris Lab, everyone in the lab has made my time at AHRI incredibly memorable. The advice that individuals have given me over past the year and a half regarding the next steps in my career as a junior scientist has been invaluable, and I look forward to collaborating with them in the near future.

Dr. Henrik Kløverpris, thank you so much for giving me the opportunity to be your MMedSci student. I have learnt so much from being in your lab and I hope I may be a future collaborator of yours. I look up to you immensely, and I hope to follow in your footsteps. To Dr. Alasdair Leslie, thank you for every bit of advice and support. I also hope to collaborate with you in the near future. Coming to AHRI and being in your guys' lab has been one of the best decisions I have ever made in my life.

To my parents, your endless love and support throughout my life has given me the opportunity to pursue my dreams. For this, I cannot thank you enough. I hope my achievements reflect how grateful I am.

TABLE OF CONTENTS

LIST OF TABLES AND FIGURES

CHAPTER 1

CHAPTER 2

ACRONYMS

AIDS	Acquired Immunodeficiency Syndrome
HIV	Human Immunodeficiency Virus
ART	Antiretroviral therapy
PLWH	People living with HIV
ILC	Innate Lymphoid Cell
CLP	Common lymphoid progenitor
NK	Natural Killer
T-bet	T-box transcription factor 21
IFNγ	Interferon γ
TNFα	Tumor Necrosis Factor α
GATA-3	GATA binding protein 3
RORγt	RAR-related orphan receptor γ
AHR	Aryl hydrocarbon receptor
LTi	Lymphoid Tissue inducer
SIV	Simian Immunodeficiency Virus
FFPE	Formalin-fixed paraffin-embedded
scRNA-seq	Single cell RNA sequencing
F-IHC	Fluorescent immunohistochemistry
cILC3s	Conventional ILC3s
GC	Germinal centres
GI	Gastrointestinal
DEGs	Differentially expressed genes
IPA	Ingenuity Pathway Analysis
PBMCs	Peripheral blood mononuclear cells

CHAPTER 1: INTRODUCTION

Acquired Immunodeficiency Syndrome (AIDS) continues to be a major global health problem since it was first recognized in 1981[1], where five cases of pneumonia were reported. Within two years, the causative agent responsible for AIDS was identified and isolated from AIDS patients, namely: the Human Immunodeficiency Virus (HIV)[2,3]. Since the start of the pandemic, HIV has claimed 36.3 million lives[4] from a total of 79.3 million people who have become infected with HIV to date[5]. In 2020, there were 37.7 million individuals living with HIV globally[4], of which over two thirds (25.4 million) live in Africa[4] and 7.8 million live in South Africa[6], the country with the highest number of people living with HIV (PLWH) in the world. KwaZulu-Natal is the worse afflicted province in South Africa with 27 % prevalence among adults aged between 15-49 years old, as presented by the most recent HIV Impact Assessment Summary in 2018[7]. A study from 2019[8] published the most detailed map ever of HIV prevalence in sub-Saharan Africa (Figure 1) which highlights the eastern regions of South Africa, most notably KwaZulu-Natal, which is where our study cohort is located.

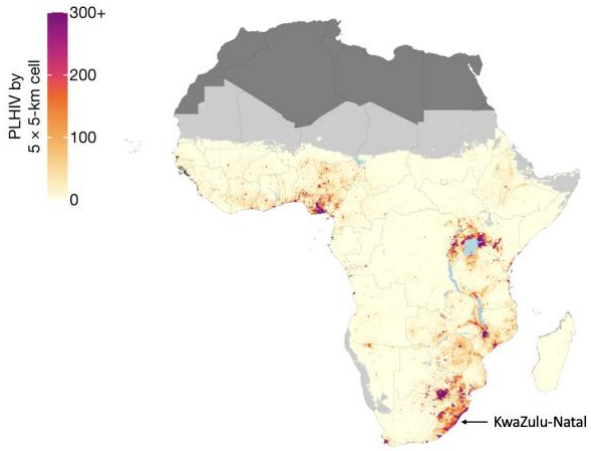

Figure 1. HIV prevalence in sub-Saharan Africa as of 2019[8]. PLHIV, People living with HIV.

HIV treatment

HIV infection remains incurable, as we still lack effective vaccines and curative treatments, but since the identification of the virus in 1983 there has been significant progress in its treatment and prevention. This progress can be attributed most notably to antiretroviral therapy (ART), along with social outreach

and education. These measures effectively control HIV replication, prevent the development of AIDS, reduce the risk of transmission, and decline the mortality rate among PLWH[9]. While ART treatment has been able to prolong life, reduce infections every year, and save millions of lives through preventing AIDS related deaths (Figure 2), ART does not cure HIV[10].

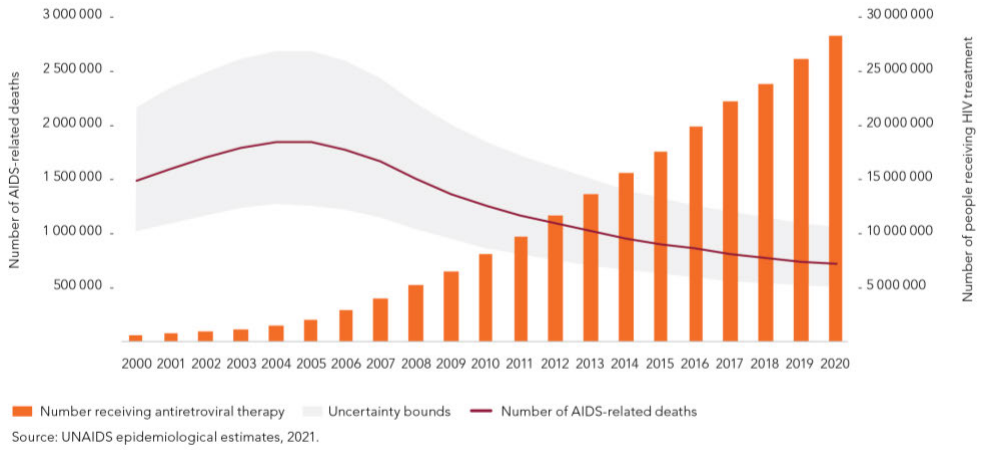

Figure 2. Number of AIDS-related deaths and people receiving HIV treatment globally, 2000 to 2020[5].

Continued ART adherence and access to ARTs are problematic, but more so is the long-term adverse effects of ARTs, which includes diabetes, bone loss, weight gain, kidney dysfunction and atherosclerotic cardiovascular disease[11]. Furthermore, it is not sustainable to expect individuals to maintain faultless ART adherence throughout their lifetime, especially when access to ARTs is limited in poor and socially disadvantaged areas. It is therefore critical that we investigate how to achieve cure.

HIV reservoirs and lymph node pathology

A major barrier to cure is the viral reservoir which consists of CD4 expressing immune cells that contain stably integrated HIV DNA which persists despite ART treatment[12,13]. These cells are found in various tissue compartments, which include the central nervous system[14], the gut[15], the genital tract[16], latently infected T-cells in the blood[17], and lymph nodes (LNs)[18]. LNs play a central role in many immune system functions since their architecture supports many complex interactions among various cell types involved in building an immune response to an invading pathogen[19]. During HIV infection, LNs become increasingly fibrotic, smaller in size, and less functional[19]. Immune responses in LNs become

dramatically impaired from HIV infection[19], contributing to the progression of AIDS. It is therefore critical to probe what impact HIV may have on various cell subsets within LNs as it could lead to the identification of novel immune responses that could contribute to eradicating the viral reservoir, and thus taking a step closer to achieving cure.

Innate lymphoid cells

Innate lymphoid cells (ILCs) are a heterologous group of mainly tissue-resident lymphocytes (Figure 3) which lack the rearranged antigen receptors of adaptive immune cells and therefore cannot respond directly to antigen presentation[20]. Tissue resident ILCs can respond immediately to invading pathogens and initiate subsequent immune responses at the site of infection[21], which has given them the title of 'sentinels' of the immune system. ILCs are grouped into either cytotoxic ILCs (exclusively NK cells) or helper ILCs which are the innate counterparts to either CD8+ T cells or CD4+ T-cells, respectively. There are three distinct groups of helper ILCs which are distinguished by the cytokines that they secrete, and their marker transcription factors. ILC1s, which mirror CD4+ T helper 1 (Th1) cells, express the transcription factor T-box transcription factor 21 (T-bet) and release interferon γ (IFNγ) and Tumor Necrosis Factor α (TNFα), functioning to eliminate intracellular pathogens. NK cells share similar features with ILC1s, but they additionally express the transcription factor EOMES and can produce cytolytic and cytotoxic granules, such as perforin and granzymes[22]. ILC2s mirror CD4+ T helper 2 (Th2) cells and express GATA binding protein 3 (GATA-3) and secrete IL-4, IL-5, IL-9, and IL-13, which function to eliminate large extracellular parasites and allergens. ILC3s, mirroring CD4+ T helper 17/22 (Th17/22) cells, express transcription factors RAR-related orphan receptor γ (RORγt) and produce IL-22 and IL-17. A major role for ILC3s is to eliminate extracellular pathogens and react to IL-23 and IL-1β stimulation from myeloid innate immune sensors. Following tissue damage, cellular debris, microbes and dying cells must be removed for tissue repair to commence, a process driven by the type 3 immune response, which involves ILC3s[20]. ILC3s therefore play a role in tissue repair and protection from tissue damage. In particular, epithelial barriers are reinforced by type 3 responses in order to resist damage by microbes in the gut. IL-22, produced mainly by ILC3s, induces epithelial cells to express anti-bacterial peptides as well as antiviral proteins and protects the epithelial barrier cells and stem cells from apoptosis through IL-22's pro-proliferative action[20]. Lymphoid Tissue inducer (LTi) cells are essential for embryonic lymphoid tissue formation during embryogenesis, however their role in adults is unclear[23]. In mice studies in LNs, ILC1s have been linked to stimulation of macrophages during viral infections[24]. ILC2s have been implicated in the induction of Th2 responses[25,26] and ILC3s to antigen presentation to CD4+ T-cells[27]. The role of helper ILCs in human LNs, however, is unknown and no human studies to date have been conducted to investigate their function in LNs[28]. ILC3s are the main helper ILC subset in LNs, which is why I chose to study this ILC subset [29]. To the best of my

knowledge, not only do no studies exist on ILCs in LNs from PLWH, but not studies investigate the impact of HIV infection on ILCs in LNs from PLWH.

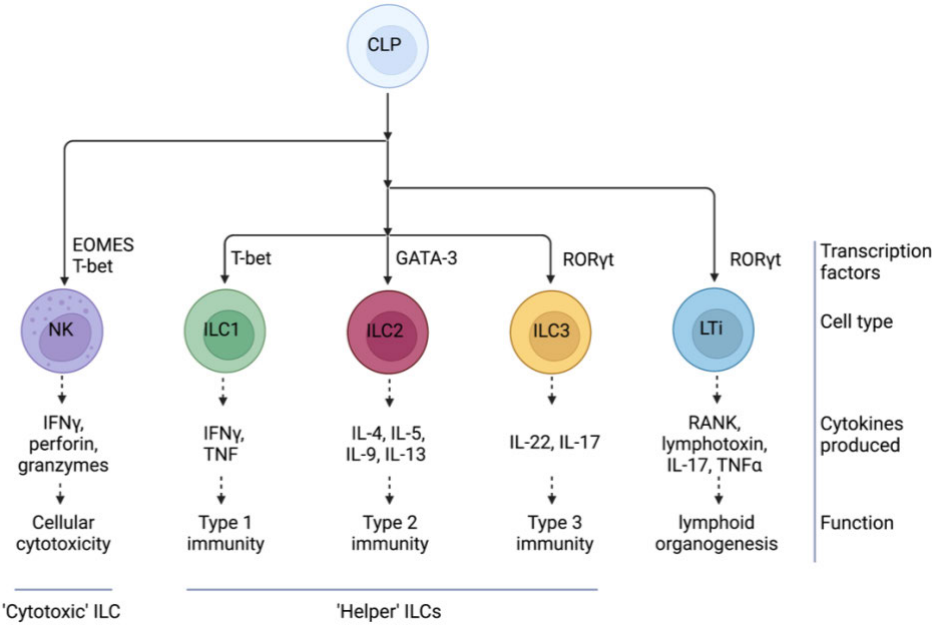

Figure 3. Human ILC subsets. Schematic diagram incorporates ILC subset marker transcription factors, secreted cytokines, and immune function (adapted from[20]). CLP: Common lymphoid progenitor. LTi: Lymphoid tissue inducer cell. Image created using BioRender.com.

ILCs and HIV/SIV infection

Because ILCs, particularly ILC3s, play instrumental roles in maintaining gut integrity, repair, and tissue remodeling[30–33], it is likely that these cells are critical players in the pathophysiology of HIV/SIV disease. During SIV-infection in rhesus macaques, it was shown that ILC3s in mucosal tissues are depleted or otherwise dysfunctional during infection[34–36]. Functionally, ILC3s from SIV-infected animals took on a more cytotoxic phenotype and produced greater quantities of TNFα and IFNγ but reduced levels of IL-17[37]. This was also found in LNs during pathogenic SIV infection[38]. This cytokine profile suggests that lentivirus infection may convert ILC3s into ILC1s, as has been previously described for mice[39]. In PLWH, our group showed that all ILC groups in blood were depleted during HIV infection, unless treatment was initiated during early acute infection[40] and that ILCs were depleted during paediatric HIV infection in the tonsils of children[41]. There are few studies investigating ILCs in human subjects, let alone the impact of HIV infection on ILC3s in human LNs, which makes this study a first of its kind.

ILC 'plasticity'

The ILC subsets experience 'plasticity', which has been extensively studied in the T helper cell subsets[42]. This phenomenon reflects a broad ability of cells to change their trajectory, functions, and phenotypes in response to changes in physiological and pathophysiological stimuli[43]. One of the hallmarks of HIV and pathogenic SIV infection is the early loss of gut integrity followed by massive and rapid translocation of microbial products from the intestinal lumen into the lamina propria, blood, liver and LNs[29]. These microbial products are associated with inflammation and chronic immune activation[29], which could regulate ILC plasticity. During inflammation, it has been hypothesized that in mucosal tissues acute inflammation results in a rapid conversion of ILC3s into ILC1s, termed 'ex-ILC3s' (Figure 4)[43]. This process of transdifferentiation between ILC3s to ILC1s occurs in response to IL-12 and IL-1ß stimulation. This agrees with what has been found in SIV infected animals[37] and in mice[39], as mentioned previously, where infection leads to ILC3s taking on a more cytotoxic phenotype, demonstrative of an 'ex-ILC3' phenotype. *In vitro* experiments addressing this model suggest that subsets of macrophages and/or dendritic cells may help drive these conversions, which is yet to be validated[44] (Figure 4). The transcriptional networks that control this plasticity depend on the expression of the controlling transcription factors, such as T-bet (for ILC1s and NK cells), GATA-3 (for ILC2s) and RORγT (for ILC3s)[43]. These suggest that the inflamed LN microenvironment during HIV infection may convert ILC3s into 'ex-ILC3s'. This hypothesis will be explored in this dissertation.

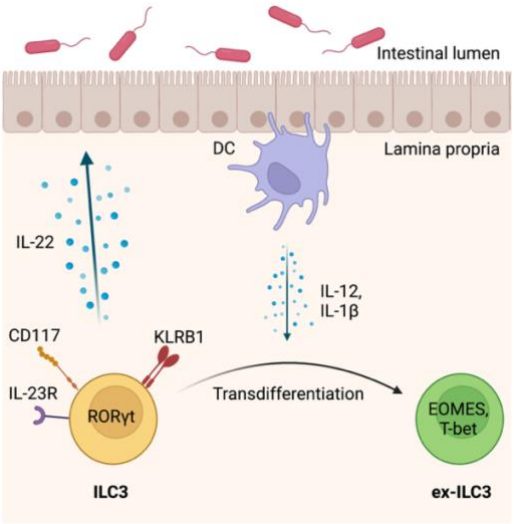

Figure 4. Schematic diagram showing the transdifferentiation of ILC3s to ex-ILC3s in the gut. This process is hypothesized to be driven by a proinflammatory tissue microenvironment (adapted from[43])**.** Image created using BioRender.com.

Study aim and hypotheses

HIV infection leads to disruption of the LN architecture through sustained inflammation and tissue fibrosis[19,45]. Since ILCs, particularly ILC3s, play instrumental roles in maintaining gut integrity, repair, and tissue remodeling[30–33], it is likely that ILC3s are involved in the immune response during HIV infection. These highlight a knowledge gap where the role that ILC3s may play in LNs, with or without HIV infection, is unknown. The next generation of ILC research will be focused on therapeutic interventions targeting ILCs. Therefore, it is necessary to know how ILCs respond in HIV infected tissue, which will be a starting point for subsequent investigation into therapeutic interventions. Furthermore, since there is a global push to get all PLWH on ARTs, it is critical that we understand the impact that HIV has on the immune system in virally suppressed patients, where sustained inflammation continues. Therefore, in this thesis, I set out to investigate the impact of HIV infection (suppressed) on ILC3s in human LNs.

Aim:

1) Investigate the impact of HIV infection on ILC3s in LNs from treated and virally suppressed PLWH.

Hypotheses:

i. ILC3s participate in the immune response during HIV infection.

ii. HIV infection drives the transdifferentiation of ILC3s into 'ex-ILC3s', due to the highly proinflammatory LN microenvironment.

Methods overview

To achieve the aim and to test the hypotheses, I utilized single cell RNA sequencing (scRNA-seq) analysis and fluorescent immunohistochemistry (F-IHC) techniques. scRNA-seq data was obtained using the Seq-Well platform[46], which allows for high-throughput RNA sequencing of thousands of single cells in parallel from low-input samples. Since ILCs are rare cell types, CD3+ and CD19+ cells were excluded prior to the Seq-Well protocol using cell sorting in order to enrich for ILCs. F-IHC is a method which uses antibodies to identify certain antigens in a tissue sample. This means that if certain antigens are markers for cell types, such as CD3 is a canonical marker for T lymphocytes, certain cell

types can be identified using F-IHC. F-IHC works well in conjunction with scRNA-seq analysis, as interesting markers brought to surface by scRNA-seq may be investigated using F-IHC.

Cohort

We utilized LN samples from a study cohort based in KwaZulu-Natal, South Africa, the epicenter of the HIV epidemic[8]. Individuals undergoing surgery from various hospitals in KwaZulu-Natal, after giving consent, had their LNs removed and transported to the Africa Health Research Institute. The study of LNs obtained for this study are approved under the protocol: Lymphoid Tissue Collection for the study of HIV and TB (BE021/13). My dissertation has been approved as a sub study of the aforementioned protocol, titled: Lymphoid Tissue Collection for the study of HIV and TB (BREC/00003988/2022) (Appendix).

This dissertation explores for the first time the impact of HIV infection on ILC3s in human LNs. Chapter 1 constitutes the literature review, knowledge gaps, aims and hypotheses, methodologies and the cohort utilized. Chapter 2 constitutes a manuscript titled, *Single-cell transcriptional profiling of lymph node resident ILC3s during HIV infection reveals links to fibrosis and cytotoxic ex-ILC3s*. Lastly, Chapter 3 constitutes the discussion/synthesis, which summarizes findings from Chapter 2 and includes future work to build on from this study.

CHAPTER 2: SINGLE-CELL TRANSCRIPTIONAL PROFILING OF LYMPH NODE RESIDENT ILC3S DURING HIV INFECTION REVEALS LINKS TO FIBROSIS AND CYTOTOXIC EX-ILC3S

Abstract

People living with HIV (PLWH) develop extensive fibrosis and collagen deposition throughout their lymphoid tissues not reversed by antiretroviral therapy (ART). Innate lymphoid cells (ILCs) play essential roles in tissue homeostasis and repair, however, no studies exist on ILCs in lymph nodes (LNs) during HIV infection. We hypothesized that ILCs are modulated by HIV infection and are involved in the subsequent immune responses. We obtained fresh celiac, cystic, bile, falciform, common hepatic and mesenteric LNs immediately after gastrointestinal surgery from patients recruited from areas in KwaZulu-Natal, South Africa – home to the highest HIV prevalence in the world. LNs from PLWH receiving ART exhibited extensive collagen deposition compared to uninfected controls characteristic of HIV-infected LN pathology. Single-cell transcriptional profiling revealed activation of the dominant ILC3 subset during HIV infection, suggesting ILC3s are directly involved in the HIV immune response. HIV-infected LNs expressed more heterogenous ILC3 subsets, including 'ex-ILC3s'. We found signatures suggesting that HIV infection induces terminal differentiation of homeostatic ILC3 populations, whereby an ex-ILC3 population becomes distinct and may contribute to a type 1 immune response. Since HIV infection leads to sustained inflammation in LNs, this terminal differentiation and emergence of ex-ILC3s may be irreversible. Moreover, we found elevated levels of TGFβ production by ILC3s during HIV infection which may suggest that these cells play a role in fibrosis formation, directly or indirectly, through fibroblast-induced collagen deposition. Here, I performed the first single-cell analysis of ILCs in HIV-infected LNs and identified ILC3s as potential contributors to LN fibrosis, a major pathological consequence of HIV infection that warrants further investigation.

Introduction

HIV continues to be a major global health burden, having claimed around 36.3 million lives[1] since it was first identified in 1983[2,3]. Antiretroviral therapy (ART) has been revolutionary in that individuals are able to effectively control viral replication which prevents the development of AIDS, reduces the risk of transmission, and declines the mortality rate among people living with HIV (PLWH)[4]. Despite

this revolutionary treatment, HIV to date remains incurable. A major barrier to the complete eradication of HIV is the persistence of the viral reservoir which is made up of CD4+ cells with integrated viral DNA that persists despite ART treatment[5,6]. These viral reservoirs can occur in several sites throughout the body which include the central nervous system[7], the gut[8], the genital tract[9], latently infected T-cells in the blood[10], and lymph nodes (LNs)[11]. Studies have shown that LNs, particularly the follicular and germinal center (GC) areas, as being major sites for viral replication and establishment of the viral reservoir[11–15]. LNs pay a central role in many immune system functions since their tissue architecture supports a multitude of complex intercellular interactions involved in building an immune response to an invading pathogen – which results in the generation of an adaptive immunity[16]. During HIV infection, the function of the LN is disrupted[16]. Lymphadenopathy has been recognized to be part of the clinical syndrome of HIV infection since the beginning of the HIV pandemic[17,18]. HIV/SIV infection induces collagen deposition in LNs, which is progressive and cumulative[19], and distorts the follicular architecture[20]. LNs become increasingly fibrotic, smaller in size, and dysfunctional as infection progresses and as circulating CD4+ T-lymphopenia becomes more pronounced[16]. Lymphoid tissue fibrosis persists in all HIV-infected individuals, including those on ARTs[21]. Indeed, among persons who start ARTs, the magnitude of fibrosis predicts inversely the magnitude of CD4+ T-cell restoration in peripheral blood[22], highlighting their importance in a functioning immune system. HIV infection leads to persistent local inflammation and altered tissue architecture that impairs both effective adaptive and innate immune responses[16]. Innate lymphoid cells (ILCs) are rare lymphocytes that lack rearranged antigen receptors and are hypothesized to be the innate counterparts of T helper cells[23]. ILCs are grouped into either cytotoxic ILCs or helper ILCs, the former encompassing only Natural Killer (NK) cells, which mirrors CD8+ T-cells. Within the helper ILCs there are three main subsets. ILC1s, which rely on the transcription factor T-box transcription factor 21 (T-bet) and produce interferon γ (IFNγ) and Tumor Necrosis Factor α (TNFα). ILC2s, which depend on the transcription factor GATA binding protein 3 (GATA-3) and produce interleukin-5 and interleukin-1. Finally, ILC3s, which require the transcription factor RAR-related orphan receptor γ (RORγt) and secrete interleukin-17 and interleukin-22 (IL-22)[23]. Because ILCs, particularly ILC3s, play instrumental roles in maintaining gut integrity, repair, and tissue remodeling[24–27], it is likely that these cells are critical players in the pathophysiology of HIV/SIV disease. During adult HIV infection, our group found irreversible depletion of ILCs from the blood unless ARTs were initiated during the early stages of infection[28]. Subsequently, the loss of ILCs was shown to be directly linked to HIV-induced inflammatory cytokines[29]. In tissue studies, SIV-infection models showed that ILCs depleted up to four fold and are dysfunctional at gut mucosal tissues[30–32]. They also exhibited elevated levels of apoptosis and cytotoxic phenotypes and were found to not only be depleted in the gut[30,32], but also the oral mucosae[33] and LNs[34]. Our group also showed that ILCs are depleted in tonsils, also a secondary lymphoid tissue, of children infected with HIV since birth[35], and the remaining ILCs exhibit increase activity despite ART treatment. However, the impact

of HIV infection on ILCs in LNs remains unknown. ILCs show a fair degree of fluidity between subgroups, a phenomenon known as 'plasticity'[36,37]. During inflammation, it has been hypothesized by Bal *et al* that in mucosal tissues, where ILC3s are the main ILC population under homeostatic conditions, acute inflammation results in a rapid conversion of ILC3s into ILC1s, termed 'ex-ILC3s'[37]. This process of transdifferentiating between ILC3s to ILC1s occurs in response to IL-12 and IL-1β, the latter being a hallmark cytokine of a highly proinflammatory microenvironment. In human tonsils, ILC3 to ILC1 transdifferentation has been observed[38], however, it is currently unknown what the impact HIV infection has on ILC plasticity in human LNs. This study, a first-of-its-kind, specifically investigated the impact of HIV infection on ILC3s in LNs from HIV positive (suppressed) compared to HIV negative participants. Here, I set out to investigate whether ILC3s participate in the immune response in LNs following infection by HIV and whether infection may drive ILC3s to ex-ILC3s. My data show that ILC3s may contribute to LN fibrosis during HIV infection through the action of TGFβ. Although pathological, this hints their participation in an immune response. Furthermore, my results suggest that HIV infection may drive ILC3 to ILC1 transdifferentation which I hypothesize is due to the inflamed LN microenvironment.

Results

Lymph node collection from PLWH

HIV infection precipitates CD4+ T-cell depletion and chronic inflammation[39] which impairs secondary lymphoid tissue, such as promoting fibrosis in LNs[40], which subsequently weakens effective immune responses[16]. To study the impact of HIV infection on ILC3s in LNs, we obtained discarded surgical material from gastrointestinal wards from hospitals around Durban, South Africa. Participants underwent open surgery for a multitude of reasons, listed in Table 1, whereby LNs were excised and transported to the Africa Health Research Institute for downstream analyses.

Table 1: Clinical parameters of participants utilized for single-cell RNA-sequencing.

PID	Lymph node type	Age (years)	Sex	Race	HIV status	ART status	ART Medication	Reason for procedure	Global Viral Load (cps/mL)	Global CD4 count (cells/μL)
022-09-5025	Mesenteric	38	Female	Indian	Positive	Yes	OAT	Jejunostomy	<20	741
022-09-5046	Cystic Duct	Unk	Male	Unk	Positive	Yes	Unk	Unknown	<20	752
022-09-5050	Falciform	35	Male	Black	Positive	Yes	OAT	Hepaticojejunostomy	<20	812
022-09-5056	Common Hepatic	18	Male	Black	Positive	Yes	Unk	Adrenalectomy	<20	800
022-09-5058	Celiac	23	Female	Black	Negative	N/A	N/A	Routine surgery	N/A	N/A
022-09-5059	Bile Lymph	36	Female	Black	Negative	N/A	N/A	Routine surgery	N/A	N/A
022-09-5061	Common Hepatic	55	Male	Indian	Negative	N/A	N/A	Routine surgery	N/A	N/A
022-09-5063	Celiac	32	Male	Black	Positive	Yes	OAT	Routine surgery	200000	402

N/A, not available
PID, participant identification number
OAT, Odimune/Atrioza/Tribuss
Unk, unknown
No participant had TB history

Severe collagen deposition in lymph nodes from PLWH

In the study cohort, I identified increased collagen deposition in an HIV-infected LN compared to an HIV negative LN (Figure 1A) and is consistent with irreversible fibrosis previously shown to be implicated in persistent immune dysregulation[20] that ultimately contributes to immunodeficiency leading to AIDS[41]. Thus, the samples exhibit characteristics of HIV-induced fibrosis and indicate that our cohort is relevant to study the impact of these changes on ILCs.

ILC3s are the major helper ILC subset in lymph nodes

In this study I set out to investigate the impact of HIV infection on ILC3s in LNs and test the hypotheses that ILC3s participate in the immune response towards HIV infection and that the inflamed tissue microenvironment drives the transdifferentation of ILC3s into ex-ILC3s. First, I analyzed single-cell RNA sequencing (scRNA-seq) data from 7 adult LNs (4 HIV positive [virally suppressed] and 3 HIV negative, Table 1), outlined in Figure 1B. scRNA-seq was performed by flow cytometric sorting of human CD3-CD19- innate immune cells (Figure 1C) to enrich for ILCs, which were then subject to the Seq-Well protocol[42]. To focus on ILC3s specifically, I used a sub-setting strategy to isolate ILC3 cells for subsequent detailed analysis. The strategy is outlined in Figure 1D. B-cells were initially excluded from the dataset (Figure S1), after which myeloid cells were also excluded from the innate immune cell dataset based on canonical cell marker genes (Figure 1D, Figure S2)[43]. The resulting innate lymphocyte population of 2031 cells included mainly ILC3s and NK cells, and some unknown CD3D+ cells which may be T-cell contamination (Figure 1D, Figure S3). Importantly, ILC1s and ILC2s were not identified.

I used IL7R, CD117 (KIT) and IL1R1 transcripts as markers for ILC3s as previously described[37,38,44,45] (Figure S3C and D) where KIT and IL1R1 are used as core ILC3 markers differentiating them from other ILC subsets. In the innate lymphocyte dataset, cluster 3 was identified as an ILC3 population (Figure S3A). It is evident, however, that other cells expressed KIT outside of cluster 3 which I hypothesize to be ILC3s (Figure S3C). To capture all ILC3s in the innate lymphocyte dataset I extracted only KIT+ innate lymphocytes (Figure 1D). Mast cells are also shown to express KIT[43,46], however, from the innate lymphocyte dataset (Figure S3E) and from the ILC3 dataset (Figure S4C), I show that the innate lymphocyte/ILC3 datasets have very few/no cells that express FCER1A, CPA3 and HDC, which are Mast cell marker transcripts[43,46]. From this, I show that Mast cells were excluded in my dataset. Therefore, a total of 476 cells were identified in my ILC3 dataset (Figure 1D and S4), where 284 and 210 cells were from HIV positive (suppressed) and negative participants, respectively. From these results, I have shown that ILC3s are the main helper ILC population in LNs, since ILC1s and ILC2s were not identified, and that the sub-setting approach to enrich for ILC3s from my initial scRNA-seq dataset resulted in cells expressing canonical ILC3 transcripts.

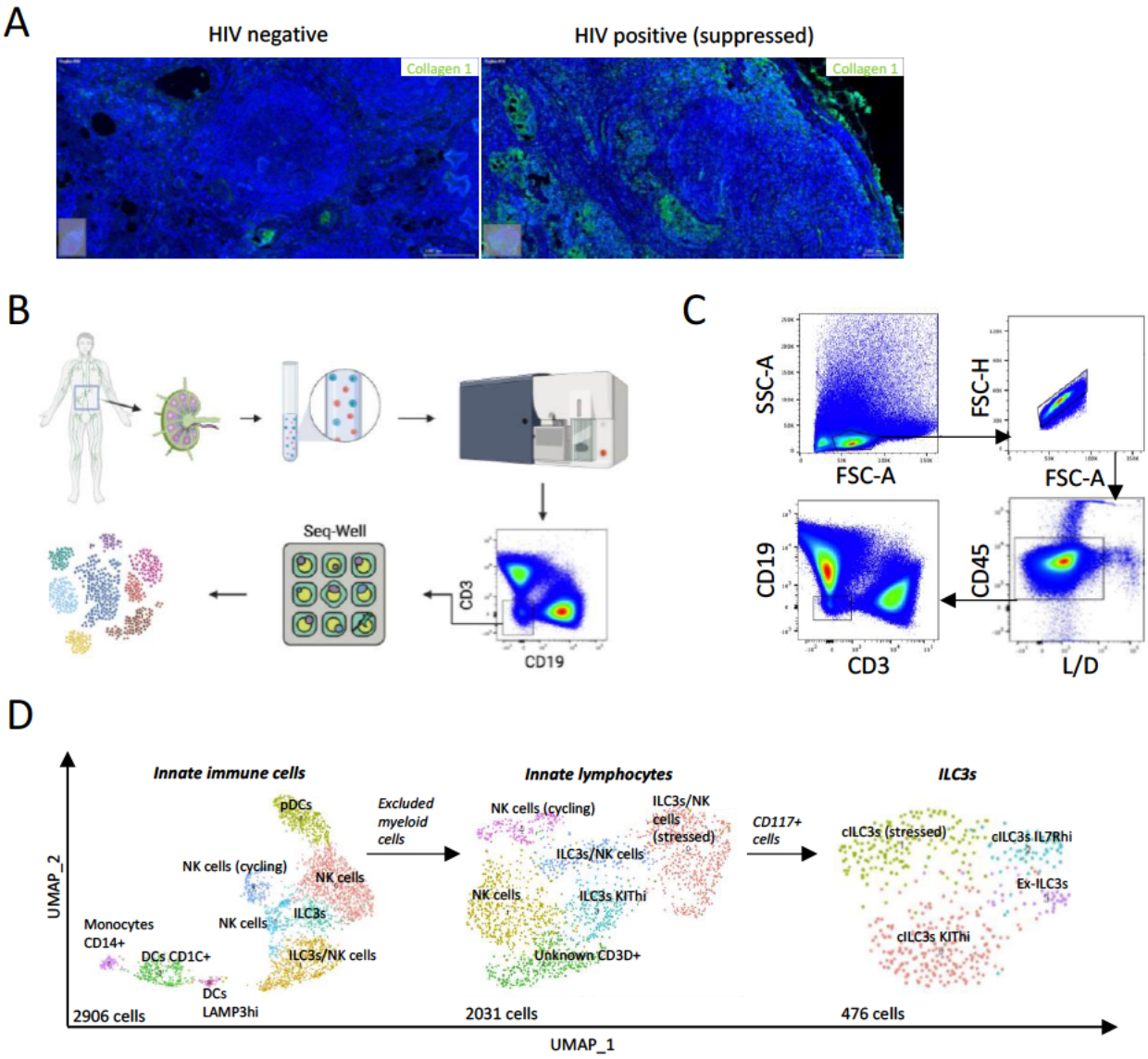

Figure 1. Single-cell transcriptional analysis of human lymph node ILC3s. A) Fluorescent immunohistochemistry of an HIV negative (participant A) and HIV positive (participant D) lymph node with Collagen 1 staining. Scale bar is 100 µm. B) Schematic of study workflow. Made using BioRender.com. C) Gating strategy used to sort for CD3-CD19- cells from human lymph nodes for subsequent application to the Seq-Well protocol[42]. D) UMAP projections demonstrating the sub-setting strategy used to isolate ILC3s from the initial single-cell RNA-seq dataset.

HIV infection regulates ILC3 plasticity

ILCs differentiate in response to external stimuli, known as 'plasticity'[37]. I set out to investigate whether I could identify ILC3 plasticity within my dataset. The ILC3 population shows a high degree of participant variability, which may be due to these ILC3s coming from various LN locations (Figure 2A). Although the dataset contains primarily common hepatic LN ILC3s (89.7 %), LN location-specific

clustering is highlighted by cluster 3, which contains primarily mesenteric LN ILC3s (Figure 2B). This shows that ILC3 plasticity may be impacted by LN location. HIV infection may also impact ILC3 plasticity since two common hepatic lymph node participants, P4 and P8, are spatially separated on the UMAP projection, of which one is HIV positive (suppressed), and one is HIV negative (Figure 2A). This possibly highlights the effect of disease state on ILC3 plasticity. Since ILCs are heavily impacted by their tissue microenvironment[36] and HIV infection leads to persistent local inflammation and altered tissue architecture[16], it is expected that we also see disease state impacting ILC3 plasticity. These results hint that LN type and HIV infection may regulate ILC3 plasticity however I cannot rule out that individual variation may also contribute.

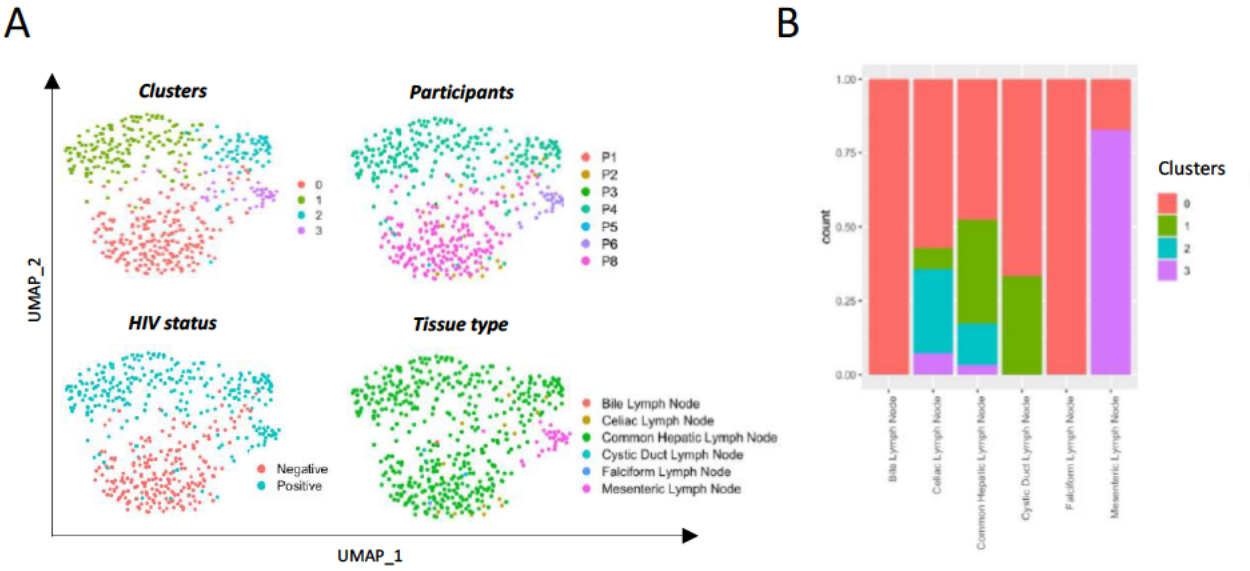

Figure 2. ILC3 plasticity may be regulated by LN type and HIV infection. A) UMAP of ILC3 dataset, separated into either cluster, participant, HIV status or tissue type. B) Bar chart showing proportion of clusters per LN type.

Higher degree of heterogeneity among ILC3s during HIV infection

All clusters, including both disease states, expressed IL7R, LTB, KIT and IL1R1, indicating that all clusters consisted of ILC3 (Figure 3C). Four clusters were identified in my ILC3 dataset of 476 cells, which includes cells from HIV positive and negative participants (Figure 3A). Interestingly, I found more prominent ILC3 subsets in human LNs during HIV infection (3 clusters consisting mainly of ILC3s from HIV positive participants) than without HIV infection (1 cluster consisting mainly of ILC3s

from HIV negative participants) (Figure 3B). When analyzing only ILC3s from HIV negative participants (Figure S5) there were two populations of ILC3s (Figure S5A). However, they did not have any significant differentially expressed genes (DEGs) between the two clusters (q-value), which is most probably why only one cluster is apparent from mainly HIV negative participants (Figure 3B). Although all clusters are present in both disease states, they are more prominent during HIV infection (Figure 3B), suggesting HIV infection leads to greater ILC3 heterogeneity or terminal differentiation. Thus, I demonstrate the identification of ILC3s in my scRNA-seq dataset and show that HIV leads to more distinct ILC3 populations which may be due to HIV driving ILC3 differentiation.

Characterizing ILC3 heterogeneity and differentiation

Of the four clusters identified within the ILC3 dataset; three conventional ILC3 (cILC3) clusters were present, since they expressed IL23R transcripts, and, interestingly, an ex-ILC3 cluster which expressed NK/ILC1 associated transcripts (Figure 3C). The ex-ILC3 population, cluster 3, expressed IKZF3 (Figure 3C), a transcription factor known as Aiolos, which has been found to downregulate RORγt expression thus polarizing ILC3 transdifferentiation towards ILC1s in the gut during inflammation[37,47], and is also a marker of ILC1s[45]. The ex-ILC3 population also expressed NK and ILC1 canonical transcripts such as EOMES, NCAM1, PRF1, T-bet (TBX21) and IFNγ (Figure 3C) and is mainly from HIV positive participants (Figure 3B). In tonsils, NK cells do not express KIT or IL1R1[44,45] – therefore it is unlikely that ILC3 dataset is populated with conventional NK cells. Therefore, I termed cluster 3 as ex-ILC3s. To further characterize the ILC3 subsets I inferred trajectory analysis using *monocle 3*[48] (Figure 3D). Interestingly, the trajectory analysis showed that the cILC3 IL7Rhi cluster and the ex-ILC3 cluster were located at the same node suggesting that they are of similar origin, which may hint that the cILC3 IL7Rhi population are transitioning to ex-ILC3s. Next, I utilized *PROGENy*[49] to characterize the signaling activity of the ILC3 subsets (Figure 3E). The ex-ILC3s and the cILC3s IL7Rhi populations showed increased stress responsive pathway activation (JAK/STAT) (Figure 3E). JAK/STAT pathway facilitates various cellular reactions to diverse forms of cellular stress, however, it is involved in a diverse range of cellular responses[50]. The stressed cILC3 and KIThi ILC3 populations also had stress response pathway activation, however through enrichment of p53 and TNFa pathways (Figure 3E). Furthermore, the ex-ILC3s are proliferative, as indicated by a cell cycling UMAP projection (Figure S4F). Although the ex-ILC3s originated from mostly one participant (P6), participant 2, 4 and 8, also had ex-ILC3s (Figure S4B). An ILC3 (NK-like) population was found when only analyzing HIV negative LNs (Figure S5A), however, there were no differentially expressed genes (DEGs) between the clusters. Indeed, although there is NCAM1 expression from the ILC3 (NK-like)

population in HIV negative participants (Figure S5B), the difference in NCAM1 expression between clusters is minimal (Figure S5D). Since the ILC3 (NK-like) population found during homeostatic conditions shares NK cell associated transcripts with the ex-ILC3/cILC3 IL7Rhi, it could hint that the ILC3 (NK-like) population terminally differentiates into ex-ILC3s/cILC3s IL7Rhi following HIV infection. In conjunction to my scRNA-seq analyses, I also investigated ILC3s by utilizing fluorescent immunohistochemistry (F-IHC) to define their spatial location in HIV negative (n=4) and HIV positive (suppressed) (n=3) formalin-fixed paraffin-embedded (FFPE) LNs (Table S1). Some tissues exhibit low CD3 expression and particular cellular structure that suggests the presence of GCs in some of the LNs. GCs express a high frequency of CXCR5[51], which I found stained in regions with low CD3 expression (Figure 3F and S9B). This suggests that low CD3 stained regions in LNs are GCs. Also, when analyzing the expression of CD117, it appeared that cells expressing CD117 were not entering the GCs in LN from an HIV negative donor (Figure 3F). CD117 is expressed on ILC3s but were found on another subset of cells co-expressing Chymase, which is a Mast cell marker[52]. From this data, I characterize for the first time ILC3s in LNs by scRNA-seq. I showed that HIV infection may be associated with the terminal differentiation of ex-ILC3s in LNs and that ILC3s predominantly reside outside of GCs, even during HIV suppressed infection.

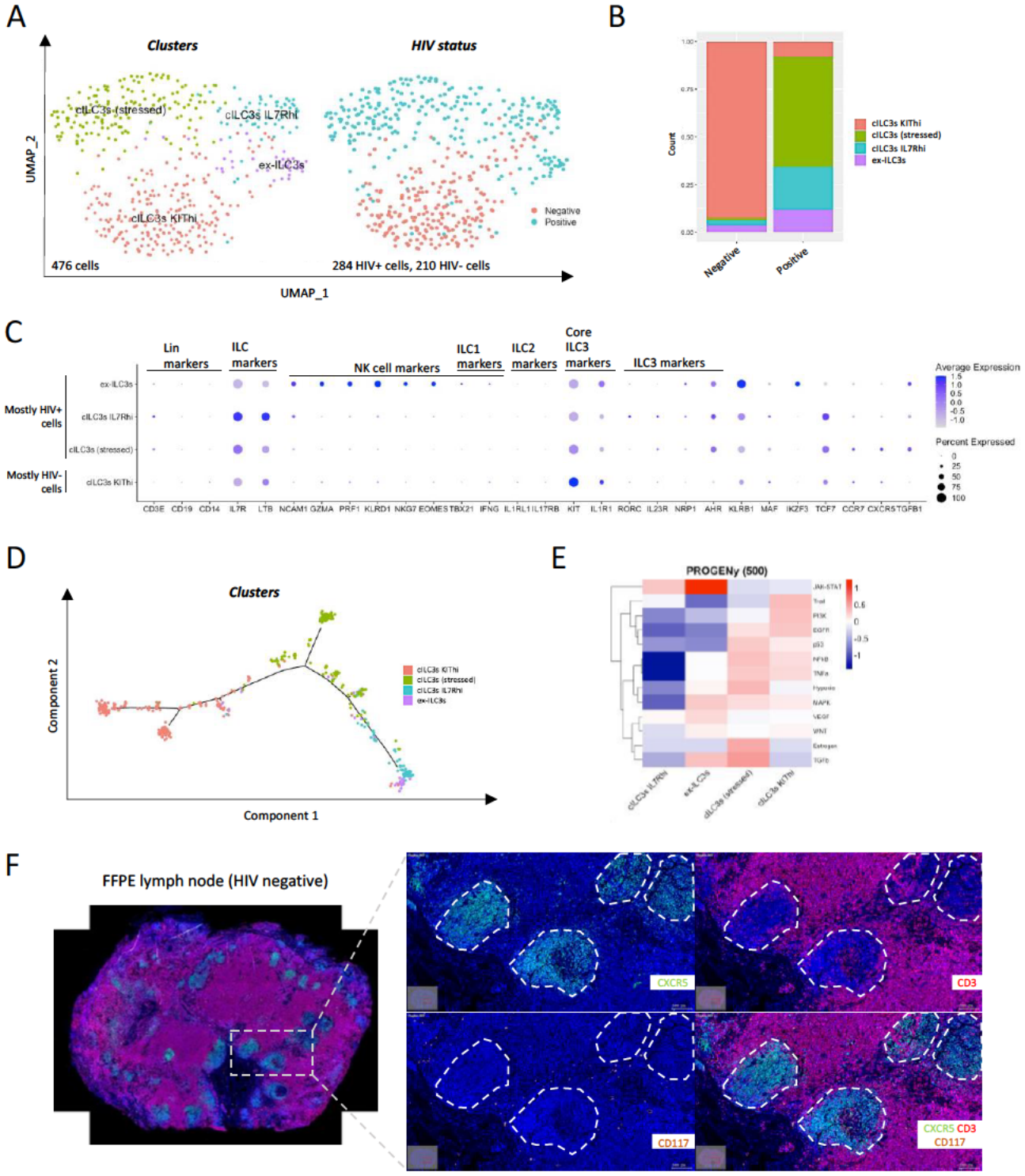

Figure 3. Characterizing ILC3s in human lymph nodes. A) UMAP projections showing either clusters or HIV status of the ILC3 dataset. B) Cluster composition per disease state. C) A DotPlot analysis of the ILC3 clusters highlighting canonical ILC transcripts and transcripts of interest. Lin, Lineage. D) A trajectory analysis concerning the ILC3 clusters. E) A *PROGENy* analysis showing pathway enrichment of the ILC3 populations. F) Fluorescent immunohistochemistry image of a human

lymph node, HIV negative (participant B), defining GC as regions lacking CD3 expression, outlined with a dashed line.

HIV-associated activation of ILC3s

Next, I compared markers of activation between ILC3s from HIV positive (suppressed) participants and HIV negative participants using global DEGs (Figure 4A). I found 502 genes were regulated by HIV infection, where 386 genes were upregulated, and 57 genes were downregulated (q value cut off at 0.05) (Figure 4B). Strikingly, I found higher levels of gene expression (nFeature_RNA) and transcript expression (nCount_RNA) from ILC3s in HIV positive participants (Figure 4A), indicating HIV infection leads to the activation of ILC3s. ILC3s from HIV positive participants also showed enrichment for transcripts associated with cytoskeletal function, TLN1 ($p=4.98x10-21$), IQGAP1 ($p=7.08x10-17$), SSH1 ($p=2.39x10-11$) and ARPC5L ($p=0.0045$), intracellular protein processing, CANX ($p=0.019$), and ribosomal RNA processing (RPL21, RPL27, RPL9, RPS27, RPS28, RPL36A), which further supports that ILC3s become activated during HIV infection whereby they change their cytoskeleton properties. Furthermore, ILC3s exhibited increased STAT3 expression from HIV positive individuals ($p=0.031$) which promotes cell proliferation and migration and further hints HIV-induced ILC3 activation. These findings suggest HIV-associated activation of ILC3s in LNs, despite suppressed viremia. This activation may contribute to ILC3 terminal differentiation and may hint that ILC3s contribute to the immune response following HIV infection.

HIV-associated stress of ILC3s

Next, I found clear upregulation of various heat shock protein and DNA repair protein transcripts during HIV infection, hinting HIV-induced stressed on the ILC3s (Figure 4B). Indeed, STK4 ($p=1.45x10-10$), a stress activated proapoptotic kinase was upregulated during HIV infection (not shown). Furthermore, a *PROGENy* analysis (Figure 4C) found the JAK-STAT pathway to be enriched during HIV infection which is a stress response pathway. Thus, global DEGs show that HIV infection is associated with ILC3 cellular stress in LNs, probably due to the inflamed microenvironment and damaged LN tissue architecture induced by HIV infection.

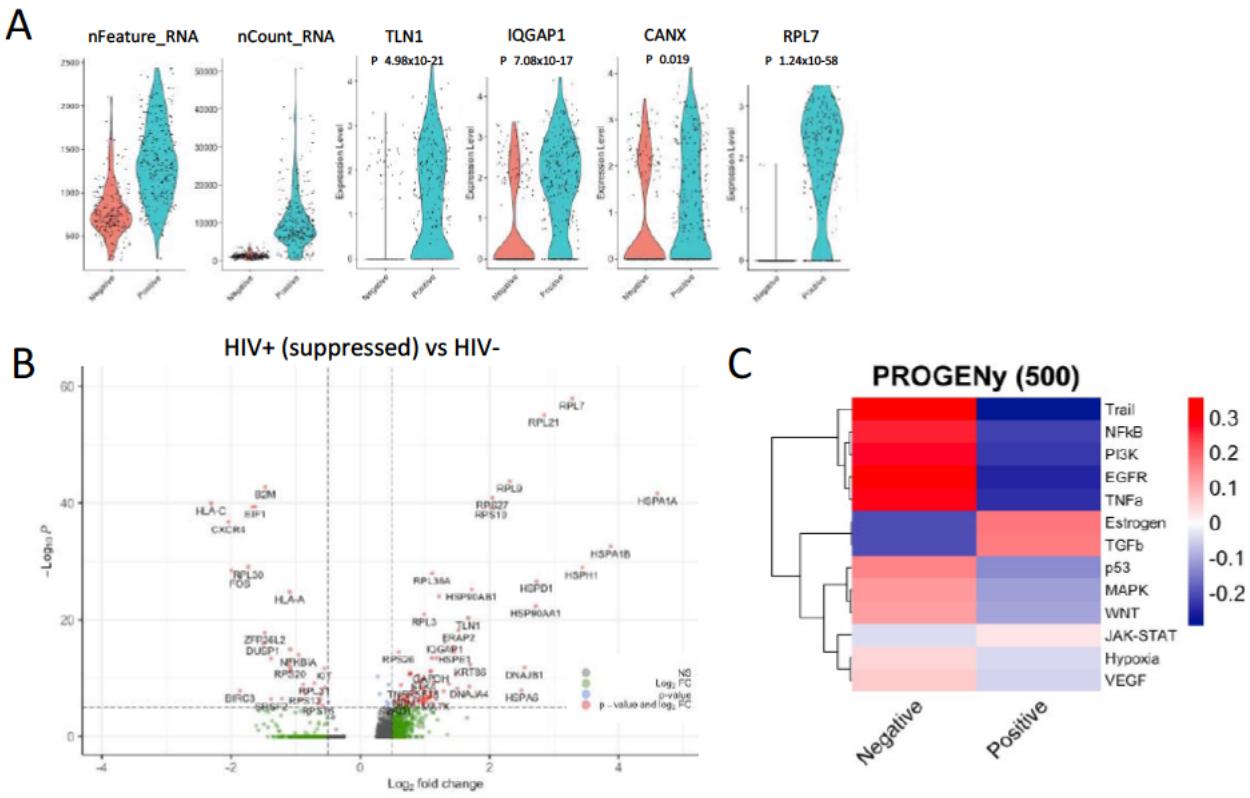

Figure 4. HIV infection may activate and induce cellular stress on ILC3s in LNs. A) ViolinPlots highlighting the total amount of genes transcribed (nFeature_RNA), RNA transcribed (nCount_RNA), and expression level of genes associated with cellular activation, compared between disease states. B) VolcanoPlot representing global DEGs from HIV positive (suppressed) ILC3s compared to HIV negative ILC3s. C) A *PROGEN*y analysis of the ILC3 dataset compared between disease states.

ILC3s remain extrafollicular, even during HIV infection

Since ILC3s are clearly impacted by HIV infection in LNs, I next sort to investigate whether HIV infection impacted their spatial location within LNs. I found that CD117+ cells, which includes ILC3s, do not enter GCs, even during HIV infection (Figure 5, Figure S8, Figure S9B). Since no CD117+ cells were found within GCs, by deduction; ILC3s do not enter GCs, even during HIV infection.

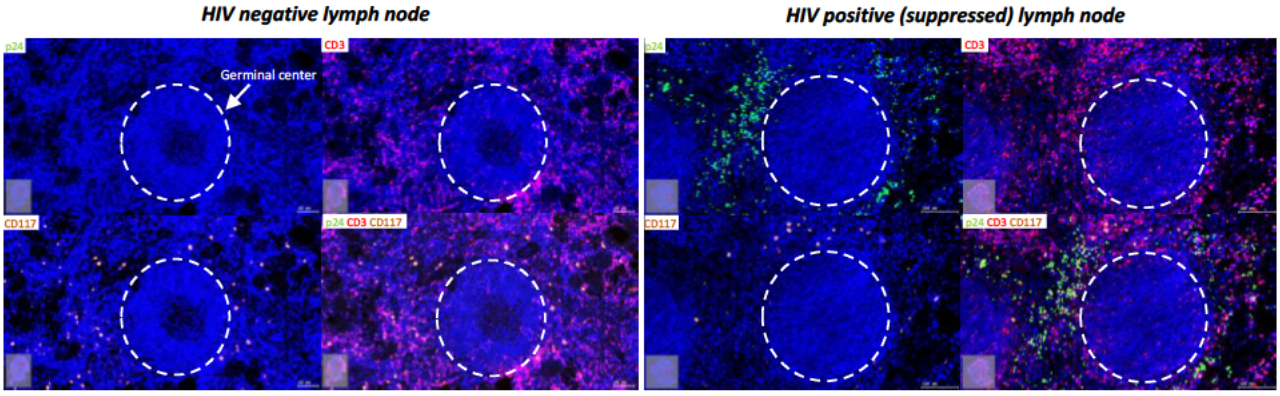

Figure 5. F-IHC images of an HIV negative and HIV positive (suppressed) LN. Tissue stained with p24 (HIV antigen), CD3 (T-cell antigen) and CD117 (Mast cell and ILC3 antigen). GCs outlined with dashed lines. Scale bar is 50 µm and 100 µm for the HIV negative and positive (suppressed) LN, respectively.

HIV infection drives ex-ILC3 differentiation

Next, using the global DEGs between disease states, I sort to investigate the hypothesis that HIV infection drives ILC3 transdifferentiation into ex-ILC3s, since I found the ex-ILC3 population to expand during HIV infection (Figure 3B). We found KIT to be significantly downregulated during HIV infection (p=2.1x10-12), which has previously been found to be characteristic of the differentiation of ILC3s to ILC1s[38,47] (Figure 6A). IKZF3, as mentioned, is crucial in the conversion of ILC3s to ILC1[37,38,47] and was upregulated in HIV infection, although did not reach significance (not shown). In tonsils, also a secondary lymphoid tissue, ILC1s were found to upregulate transcripts encoding members of the TNF receptor and TNF superfamilies[45]. TNFRSF18 (p=3.22x10-9) and TNFSF13B (p=0.014) were significantly upregulated during HIV infection in ILC3s, further hinting a conversion of ILC3s to an ILC1 phenotype (Figure 6A). Also in tonsils, it was found that when ILC3s transition to ILC1s, CD300LF, which is involved in MHC I antigen processing, is upregulated[38]. Similarly, we observe an upregulation of CD300LF in LNs from PLWH (p=3.63x10-9) (Figure 6A). ILF3, which participates in the antiviral innate immune response, is upregulated during HIV infection (p=1.18x10-5) (Figure 6A), which could infer that ILC3s can respond specifically to viral infection, hinting a type 1 immune response. ILC3s in tonsils have been shown to express transcripts encoding products involved in three key signaling pathways regulated by ligands of the receptors c-Kit, Notch and NKp44[45]. As mentioned, KIT is downregulated (p=2.095x10-12) in HIV-infected LNs. Transcripts involved in the Notch pathway, proteinase ADAM10 (p=0.010) and the intracellular signaling molecule RBPJ (p=0.0059), are upregulated during HIV infection (not shown). NKp44 (NCR2) is not differentially expressed between the disease states. This suggests ILC3s increase Notch signaling while decreasing

c-Kit signaling during HIV infection in LNs. Notch signaling was found to increase in ILC3s as they differentiate into ex-ILC3s[38] which further provides evidence that HIV infection drives ILC3s to ex-ILC3s. Lastly, the TGFβ pathway was found to increase during ILC3 to ILC1 transition in tonsils[38], which agrees with my data (Figure 4C), and confirms the hypothesis of transitioning ILC3s. The ex-ILC population also had a high proportion of cells that expressed cytotoxic associated transcripts GZMA and PRF1(Figure 6B), suggesting that ex-ILC3s are cytotoxic in LNs. To exclude potential confounding results due to the various localizations of the LN studied, I focused my analysis on DEGs between disease states from ILC3s from only common hepatic LNs to eliminate LN type variability (Figure 6C and S6) as I previously found LN type to potentially impact ILC3 plasticity (Figure 2A). Indeed, I still found a decrease in KIT expression ($p=6.53x10-12$) and an increase in CD300LF ($p=1.22x10-9$), TNF receptor and TNF superfamily expression, TNFRSF18 ($p=7.62x10-12$) and TNFSF13B ($p=0.013$), and an upregulation in the TGFβ pathway (Figure S6D and F). Furthermore, an NK-like ILC3 population was present which had upregulated NCAM1 and CD300LF transcripts (Figure S6H) which may suggest that this population is transitioning to ex-ILC3s. Again, an NK-like ILC3 population was observed when only analyzing HIV negative LNs (Figure S5A), however there were no DEGs between clusters, which hints that HIV infection leads to these populations becoming prominent. This may be inferred by Figure 6D, which shows ILC3s from only common hepatic LNs, where two populations become apparent during HIV infection but are not apparent when there is no infection, suggesting that HIV leads to the terminal differentiation of these subsets, one being an NK-like ILC3 or ex-ILC3 subset. These results suggest that HIV infection in LNs drives ILC3 differentiation into ex-ILC3s consistent with the inflamed tissue microenvironment. Thus, my results suggest HIV infection terminally differentiates ILC3s which precipitates two distinct ILC3 populations in LNs, namely conventional ILC3s and ex-ILC3s.

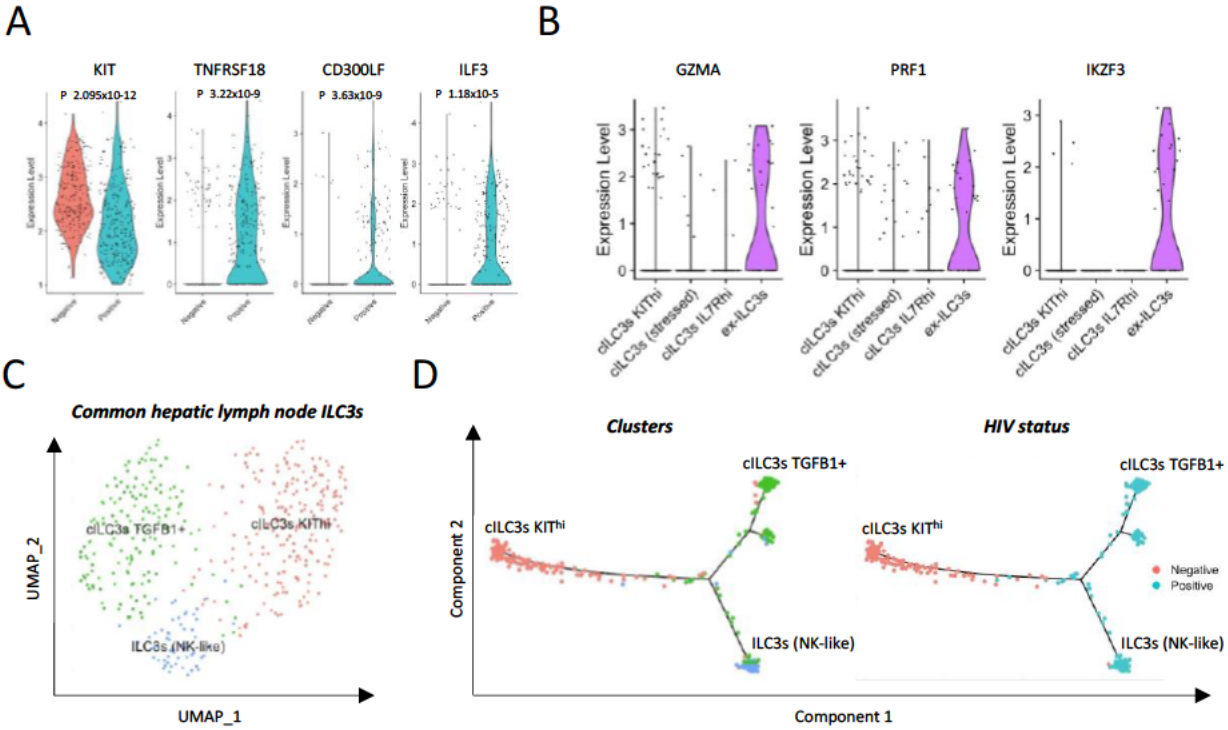

Figure 6. HIV infection drives the emergence of ex-ILC3s in LNs. A) ViolinPlots highlighting DEGs between disease states associated with ILC3 transdifferentiation and antiviral response from ILC3 dataset. B) Ex-ILC3 associated transcripts expression between clusters from ILC3 dataset. C) UMAP projection of ILC3s from the common hepatic LN dataset colored according to clusters. D) Trajectory analysis of ILC3s from the common hepatic lymph node dataset, highlighting clusters or HIV status, where two ILC3 populations emerge during HIV infection.

ILC3s may contribute to HIV-induced fibrosis

Interestingly, in the *PROGENy* analysis of the ILC3s (Figure 4C), the TGFβ pathway was upregulated during HIV infection, which is a major profibrotic factor[53]. Therefore, I next sort to investigate the role ILC3s play in HIV-induced fibrosis by probing global DEGs from ILC3s between disease states. Indeed, during HIV infection, ILC3s significantly upregulated TGFB1 expression (p=3.6x10-7) (Figure 7A) which contributes to Th17 differentiation and immune tolerance[54]. Indeed, FOS, which regulates TGFβ signaling, was downregulated during HIV infection (p=3.56x10-28) (Figure 7B). Interestingly, TGFB1 expression level were comparable across ILC3s from mainly HIV positive clusters (Figure 7C), and when just comparing common hepatic LN ILC3 clusters (Figure 7D). This suggests all ILC3 subsets upregulate TGFB1 expression uniformly rather than in a subset specific manner during HIV infection. Using Ingenuity Pathway Analysis (IPA)[55], a graphical summary was obtained, utilizing DEGs due to HIV infection, which showed various elements involved in TGFB1 upregulation (Figure S7). IL-4, a

pleiotropic anti-inflammatory cytokine that functions mainly by suppressing the proinflammatory milieu (reviewed in[56]), and NFE2L2, a transcription factor that regulates genes which encode proteins which respond to injury and inflammation[57], are involved in upregulating TGFB1 expression. These elements, namely IL-4, NFE2L2 and then subsequently the expression of TGFB1, appear to function to counteract the pathological effects of HIV-driven inflammation. This suggest that ILC3s may play a protective role in LNs where they may reduce HIV-driven inflammation and injury. Using F-IHC, we found that ILC3s (IL1R1+CD117+ cells) were positively stained for TGFβ in an HIV negative and positive LN (Figure 7E), which infers the transcripts observed in my scRNA-seq data translate into protein. Interestingly, although TGFβ contributes to immune tolerance[54], it also stimulates fibroblast to deposit collagen, thus contributing to fibrosis[40,53]. This suggests that ILC3s, being a source of TGFβ, probably contribute to HIV-induced fibrosis. In order to appreciate the level of TGFB1 expressed from our ILC3s, I next compared their level of TGFB1 expression to TGFB1 expressing cells from a LN dataset which was also obtained using the Seq-Well protocol, however, no prior sorting was undertaken, and so I titled this dataset TGFB1_UT (UT: un-touched, or not sorted). This dataset should contain all immune cells found in LNs expressing TGFB1 that do not express more than 5% mitochondrial genes (strategy outlined in Figure 7F). I found that my TGFB1 expressing ILC3s (ILC3_ILCenriched, 23.3 % of ILC3 population) expressed, on average, less TGFB1 than total TGFB1 expressing cells ($p=0.0029$) (Figure 7G). However, A *PROGENy* analysis showed that the TGFβ pathway enrichment were not exceptionally different between the datasets (Figure 7H). These results show that ILC3s are a source of TGFβ during HIV infection in LNs and therefore may contribute to HIV-induced fibrosis.

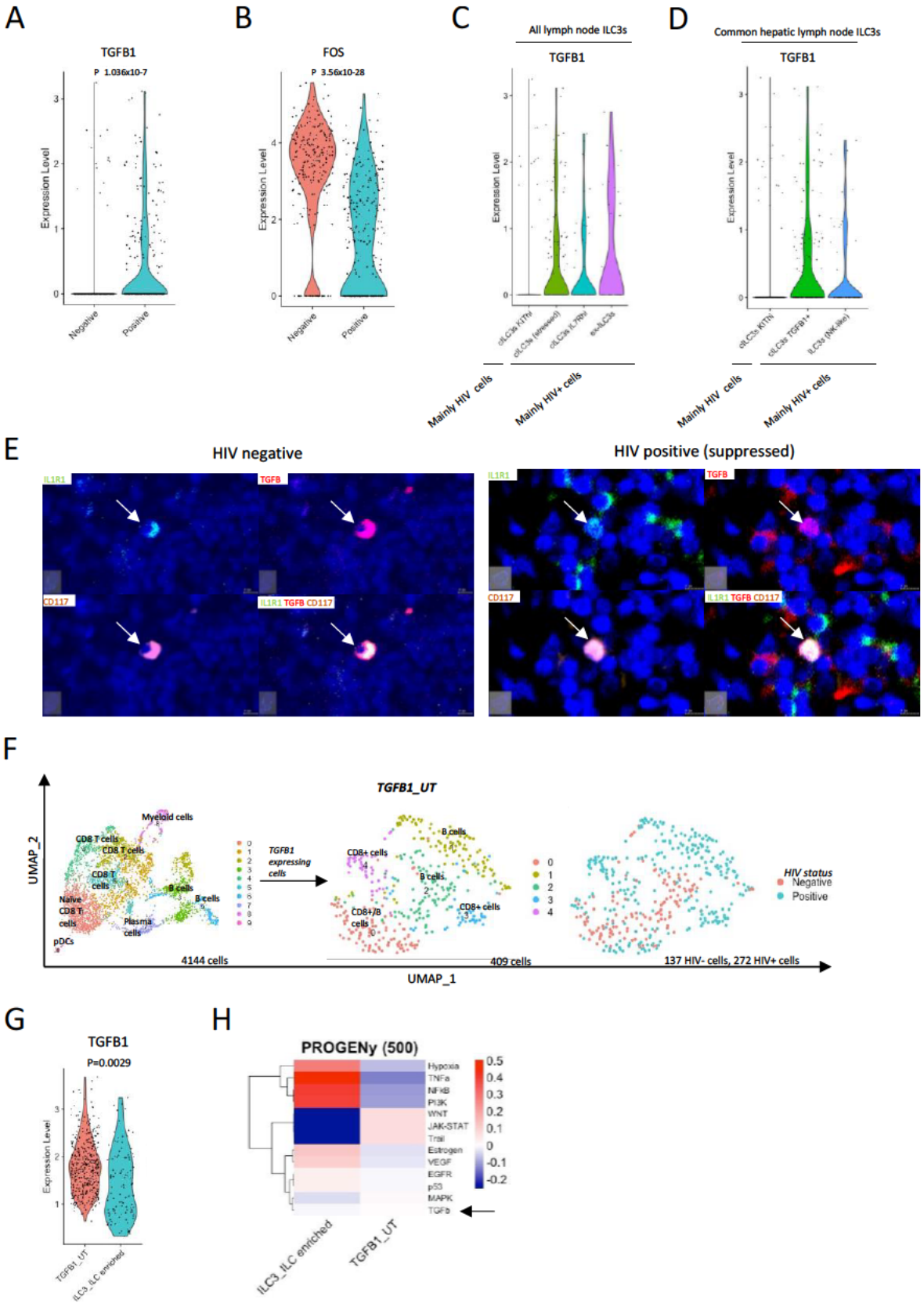

Figure 7. ILC3s secrete TGFβ, which may contribute to HIV-induced fibrosis. A) ViolinPlots of TGFB1 and B) FOS transcript expression level, compared between disease states. C) ViolinPlot of

TGFB1 expression levels across ILC3s clusters from ILC3 dataset. D) ViolinPlot of TGFB1 expression levels across clusters from only common hepatic LN ILC3s. E) F-IHC images of ILC3s (IL1R1+CD117+ cell) which stain positive for TGFβ, in an HIV negative (participant A) and an HIV positive (suppressed) (participant D) LN. Scale bar is 5 μm. F) Sub-setting strategy used to isolate TGFB1 expressing cells from a LN scRNA-seq dataset that did not undergo cell sorting, labeled TGFB1_UT. G) A ViolinPlot comparing TGFB1 expression levels between the ILC3 dataset (CD3-CD19- sorted cells) and TGFB1 expressing cells from the LN scRNA-seq dataset that did not undergo cell sorting. H) A *PROGEN*y analysis comparing signaling pathways between the two datasets.

Viremia boosts IFN-I responses in ILC3s

Lastly, I sort to investigate whether HIV viremia has a differential impact on ILC3s compared to suppressed HIV infection using scRNA-seq analysis (Figure 8A). Only one HIV viremic participant was available for this analysis. Comparing HIV positive (viremic) to HIV negative, IFI44L (p=0.00015), an interferon induced protein, and DDX3Y (p=5.4x10x10-6), which may enhance IFNB1 expression, was upregulated (Figure 8C), suggesting a type I interferon response from ILC3s within the inflamed tissue microenvironment during viremia. Ribosomal genes in ILC3s from viremic compared to HIV suppressed participants was downregulated, suggesting that ILC3s are more active in HIV suppressed participants. An increase in ribosome biogenesis, which hints increased proliferation, suggests HIV suppressed individuals have more functional ILC3s compared to viremic individuals. This is consistent with the enrichment of the JAK-STAT pathway, a stress response pathway, in ILC3s from HIV positive (viremic) individuals compared to the other disease states (Figure 8B), as ILC3s during viremia may be under increased cellular stress which may impact their functionality. Unexpectedly, KIT is upregulated in ILC3s from HIV positive (viremic) participants compared to suppressed (p=1.74x10-6) since I expected viremia to lead to a stronger ILC3 to ILC1 differentiation. Interestingly, the TGFβ signaling pathway is enriched in ILC3s from HIV positive (suppressed) participants compared to viremic and HIV negative participants, which further suggests that ILC3s are more functional when viremia is suppressed. I observed increased HIV p24 antigen staining in an HIV positive (viremic) FFPE LN compared to other disease states (Figure S5), which suggests systemic viremia predicts increased HIV replication in LNs. From these results, we show that HIV viremia may drive a type I IFN response in ILC3s compared to suppressed HIV infection in LNs.

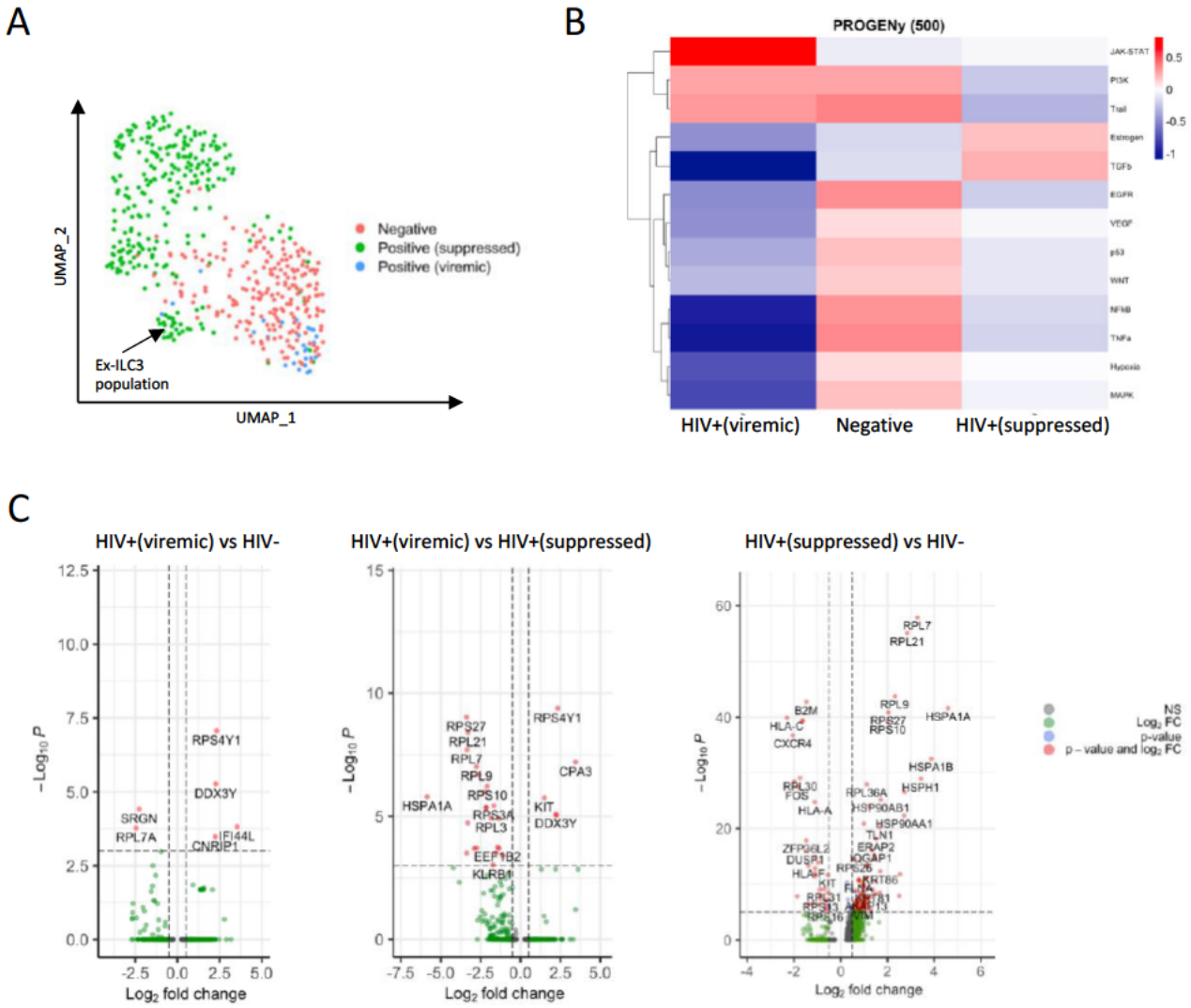

Figure 8. Comparing DEGs from ILC3s between HIV positive (viremic), HIV positive (suppressed) and HIV negative participants. A) A UMAP projection highlighting the different disease states. B) A *PROGENy* analysis comparing signaling pathways between disease states. C) VolcanoPlots, comparing differentially expressed genes between the different disease states.

Discussion

In this study, I sort to characterized ILC3s in human LNs and investigate the impact of HIV infection on these cells by employing scRNA-seq and F-IHC. I tested the hypotheses; 1) ILC3s participate in the immune response following HIV infection in LNs, and 2) the proinflammatory microenvironment, induced by HIV infection, leads to the transdifferentiation of ILC3s to 'ex-ILC3s'. I have shown that ILC3s may contribute to HIV-induced fibrosis through the action of TGFβ, where they surprisingly

may contribute to the pathology of HIV, hinting they do participate in an immune response, despite being pathological. Also, HIV infection may drive ILC3s transdifferentiation into ex-ILC3s. Interestingly, I find two distinct ILC3 populations, a conventional ILC3 population and an ex-ILC3 population, that become prominent during HIV infection.

LNs play a central role in the development of an immune response to pathogens as their architecture allows for complexed cellular interactions that lead to an effective immune response[16]. However, following HIV infection, LNs become highly proinflammatory and have impaired architecture[16,58]. In the study cohort, I identified increased collagen deposition in an HIV positive (suppressed) LN compared to an HIV negative LN, which agrees with literature[20], reflecting the clinical progression of disease and highlighting impaired tissue architecture following HIV infection (Figure 1A). My results show that ILC3s are the major helper ILC subset in LNs, which agrees with literature[59] (Figure 1D). ILCs are plastic and can transform into other ILC subsets in response to environmental stimuli[36,37]. HIV infection in LNs precipitates a sustained inflammatory microenvironment which is likely to regulate ILC plasticity. Indeed, HIV infection led to common hepatic LN ILC3s having differential spatial location on a UMAP projection separated by disease state (Figure 2A). UMAP projections cluster cells based on similar transcriptomic signatures, and so, since HIV infection led to the separation of ILC3 cells based on disease states, I hypothesize that this is support for HIV infection regulating ILC plasticity in LNs, since there is no tissue-specific bias and both participants are male. Also, LN type also seemed to impact ILC3 plasticity. However, inter-individual difference may be a driving force here and so more biological replicates are required to demonstrate the impact of HIV infection on ILC3 plasticity.

Next, I characterized for the first time ILC3s in LNs using scRNA-seq and investigated the impact of HIV infection. I found that ILC3 subset heterogeneity expands during HIV infection (Figure 3B). This suggests that the two ILC3 subsets found during homeostatic conditions (Figure S5A), which had no DEGs between them, became prominent during HIV infection, possibly due to terminal differentiation driven by HIV infection. I also found ILC3s become activated during HIV infection, which may be triggered by specific environmental cues, such as the highly proinflammatory microenvironment or cell-to-cell signaling by other immune subsets, which may be evidence that these cells terminally differentiate due to HIV infection. Interestingly, an ex-ILC3 population with cytotoxic potential emerges during HIV infection which supports my original hypothesis.

My results, as mentioned, suggest ILC3s become activated during HIV infection, even during suppressed viremia (Figure 4A). Amongst other elements, we found an increase in ribosomal proteins which is a critical feature of proliferating cells[60] and is an indicator that, during HIV infection, ILC3s become activated. Indeed, despite profound immune deficiency during HIV infection, immune activation is recognized as a characteristic of HIV infection[16]. Since LNs are viral reservoir sites[11], there

is an accumulation of HIV antigens, where viral replication is a major contributor, which subsequently leads to sustained inflammation within LNs[16]. ILCs do not express HIV entry receptors CXCR4 or CCR5 and therefore cannot be directly infected by HIV[23]. This suggests that ILC3 activation is due to the inflamed tissue microenvironment induced by HIV infection. This is also characteristic for CD4+ and CD8+ T lymphocytes during HIV infection[16]. Consistently, my data suggests that this may also extend to ILC3s. Furthermore, our group showed that ILCs are depleted in tonsils of children infected with HIV since birth[35], and that the remaining ILCs exhibit increased activity despite ART treatment. This newly generated data supports the previous findings and shows that it can be extended to the adult population. Next, I found ILC3s become stressed during HIV infection, as I found a striking upregulation of heat shock and DNA repair protein transcripts (Figure 4B), which, too, probably reflects the response to the inflamed tissue microenvironment. An upregulation of shock and DNA repair protein transcripts are normally upregulated upon an increase in temperature or mechanical stress[61]. Also, despite clear HIV-induced cellular activation and stress, ILC3s remain intrafollicular but outside the GCs as shown by my F-IHC images (Figure 5).

In agreement with my hypothesis, I found the emergence of an ex-ILC3 population in HIV-infected (suppressed) human LNs with cytotoxic potential (Figure 3A). I hypothesize this population to have terminally differentiated from an NK-like ILC3 population in response to the highly inflamed LN microenvironment following HIV infection. IKZF3, also known as Aiolos, a member of the Ikaros transcription factor family, has been implicated in the conversion of ILC3 to ex-ILC3s[37,38,47], which I find to be highly expressed in my ex-ILC3 population (Figure 6B). Aiolos binds to regulatory elements of genes that control ILC3 function, such as RORγt, thereby repressing their genes[38]. NK cells and ILC1s have overlapping transcriptional profiles, hence why they are both included in the type 1 ILC subset[23]. In the human intestine, Crohn's Disease leads to an increase in ILC1s at the expense of ILC3s, which suggests that chronic inflammation may result in the conversion of ILC3s into ILC1s[62–66]. Also, intestinal infection in mice with human immune systems lead to the rapid conversion of ILC3s to ILC1s[66]. Further studies have shown that there are intermediate populations between ILC3s and intraepithelial CD103+ ILC1s in human tonsils and the small intestine[38], where an increase in CD300LF leads to CD103+ ILC1s differentiation, as was found in my data. During SIV-infection, ILC3s took on a more cytotoxic phenotype in the oral mucosa and produced increased amounts of TNFα, IFNγ, and MIP1B[33]. Although I did not find increased expression of these cytokines, I did find an increased expression of GZMA, PRF1 and, to a lesser extent IFNγ, which are also cytotoxic (Figure 6B). Indeed, studies on patients with irritable bowel disease (IBD) have shown that ILC3s can play a pathogenic role in intestinal inflammation[67–70]. I hypothesize that, during HIV infection, NK-like ILC3s terminally differentiate into ex-ILC3s in response to the proinflammatory microenvironment to contribute to a type 1 immune response. Bal *et al* hypothesize that after resolution of inflammation, ILC1s reconvert to

ILC3s[37]. However, sustained inflammation during HIV infection[16,58] may inhibit the reconversion of ex-ILC3s back to conventional ILC3s, which means that ex-ILC3s transdifferentiation may be irreversible. Since ILCs experience cellular 'plasticity' during HIV infection, which my data suggests so, I hypothesize that the cILC3s IL7Rhi (Figure 3A) and ILC3 (NK-like) (Figure 6C) populations found during HIV infection, which expressed modest NCAM1, may be transitioning to ex-ILC3s. The NK-like ILC3 population that was found during homeostatic conditions, however, had no DEGs between the subsets which suggests that HIV infection, and therefore an inflamed tissue microenvironment, may drive this subset to terminally differentiate whereby it becomes prominent during HIV infection. This may infer that ex-ILC3s do not transdifferentiate from conventional ILC3s, but rather terminally differentiate from NK-like ILC3s during homeostatic conditions driven by HIV infection, where, following HIV infection, they become prominent (Figure 6D). HIV infection driving ILC3 terminal differentiation may be why I observe more ILC3 subsets from HIV-infected participants.

A hallmark of HIV infection is the early loss of gut integrity followed by massive and rapid translocation of microbial products from the intestinal lumen into the lamina propria, blood, LNs, and liver[39,71–73]. The IKZF3+ ex-ILC3 population was found mainly in the mesenteric LN ILC3 population (Figure 2B). I reason that the mesenteric LN becomes more inflamed during HIV infection compared to the other LN types due to its proximity to the gut. Since HIV infection leads to rapid microbial translocation from the gut, gut draining LNs such as mesenteric LNs may be exposed to higher concentrations of microbial products and thus potentially experience more inflammation than other LN types in this study. However, since the study lacked a HIV negative mesenteric LN as a control, this requires further investigation. However, as seen in the UMAP clustering (Figure 2A), I cannot rule out individual variation also contributes.

Remarkably, my results suggest that ILC3s upregulate TGFβ secretion in response to HIV infection in LNs. TGFβ is possibly best known to induce peripheral tolerance, where one of the mechanisms by which TGFβ can maintain peripheral tolerance is to maintain the survival of naturally occurring T regulatory (T-reg) cells (reviewed in[74]). However, TGFβ does has proinflammatory effects, which are best shown by its ability to drive the differentiation of Th17 T-cells in the presence of IL-6, which can promote inflammation[74]. Disruption to LNs during HIV infection, in the form of fibrosis, majorly contributes to an impaired immune system[16,20]. TGFβ is a major profibrotic factor and is central to this process[53]. LN damage following HIV infection, induced by destructive proinflammatory cytokines and CD4 T-cell depletion[22,75], may lead to a state of wound healing, which is a complexed multi-phase process, involving inflammatory cell chemotaxis, fibroblast proliferation, collagen and matrix deposition, angiogenesis and reduced matrix degradation by metalloproteinases (reviewed in[53]). Fibroblasts migrate to the wound site where they transform into myofibroblasts where, upon TGFβ

stimulation, deposit collagen. When TGFβ is overproduced there is excessive collagen and matrix deposition, resulting in organ dysfunction or failure[53], which is exactly what occurs in HIV-infected LNs[40]. A major contributor to collagen deposition/fibrosis is the presence of T-reg cells that accumulate in the LN in the context of persistent inflammation that characterizes chronic HIV/SIV infection[40,75–77]. These cells secrete TGFβ and have temporal and spatial relations to fibroblasts, and upon TGFβ stimulation, fibroblasts deposit collagen[40]. Therefore, ILC3s may also contribute to fibrosis indirectly through maintaining T-regs or by directly stimulating fibroblasts to deposit collagen. Also, I have shown that ILC3s enrich the TGFβ pathway to comparable levels as other TGFB1 expressing cells in LNs (Figure 7H). Furthermore, I used F-IHC to infer these TGFB1 transcripts are translated into protein (Figure 7E). It is unclear the relative amount of TGFβ ILC3s produce during HIV infection, however ILC3s do seem to be a source of TGFβ during HIV infection. Both ex-ILC3s and cILC3 seem to be sources of TGFβ (Figure 7C and D). Thus, it seems that ILC3s upregulate TGFβ, regardless of ILC subset, to counteract the pathological consequences of HIV, namely inflammation and injury, by inducing immune tolerance or to contribute to wound healing. However, this may be a double-edged sword, in that the consequence of TGFβ upregulation may contribute to fibrosis[16,20,53], either directly or indirectly, which leads to LN dysfunction, thus contributing to the progression of AIDS[41]. I have identified a new cellular source of TGFβ, and therefore a new potential contributor to fibrosis in LNs during HIV infection. Thus, HIV infection leads to two distinct ILC3 populations emerging, an ex-ILC3 population and a cILC3 population, which are both sources of TGFβ.

Lastly, I later included a viremic participant into the dataset and found that ILC3s from the viremic participant had an enriched type I immune response pathway, due to the upregulation of transcripts involved in type I IFN pathway, and the enrichment of the stress response JAK-STAT pathway which leads to IFN cascade signaling (Figure 8B and C). Furthermore, it is the ILC3s from HIV suppressed participants that have an enriched TGFβ pathway (Figure 8B) as well as ribosomal protein transcripts which suggests that ILC3s may be more functional in LNs during suppressed viremia than viremia (Figure 8C). TGFβ pathway enrichment may be an indicator of ILC3s participating in an immune response and ribosomal biogenesis as an indicator of proliferation or activation, which ILC3s from the viremic have compared to the ILC3s from suppressed infection. However, this is still speculative and requires further investigation.

ILCs fill a unique tissue-resident niche as first responders to infection. Here, I attempt to further understand these unique cells and their relationship with HIV in LNs. I have shown that ILC3s may become activated and probably contribute to the immune response following HIV infection, however it may be pathological. I propose that HIV infection terminally differentiates ILC3 subsets, where a distinct ex-ILC3 population emerges with cytotoxic potential. I hypothesize that HIV infection does not

transdifferentiate conventional ILC3s into ex-ILC3s, but rather ex-ILC3s terminally differentiate from NK-like ILC3s present in LNs during homeostatic conditions which may contribute to a type 1 immune response. Furthermore, ILC3s may contribute to HIV-induced fibrosis through the action of TGFβ, highlighting a novel cell type previously unknown to contribute to HIV-induced fibrosis.

Methods

Study participants

To investigate ILC3s in LNs, LN samples were obtained from individuals a part of the 'Gut-associated lymphoid tissue' study cohort, collected from local hospitals around Durban, South Africa. Participants underwent open surgery whereby LNs are excised. Participants underwent surgery for a multitude of reasons, listed in table 1. Formalin-fixed paraffin-embedded LNs were stored from the cohort collected over the years, of which 4 HIV+ (3 suppressed, 1 viremic) and 4 HIV- LNs were chosen to be used for F-IHC analysis for this study. Fresh LNs from the same cohort, received the day of surgery, were utilized for Seq-Well (described below). We obtained matched samples of peripheral blood from each participant. A portion of the peripheral blood obtained was sent to Neuberg Global Laboratories for hematological analysis whereby a pathology report was produced, where HIV viral load, SARS-CoV-2 IgG test, and CD4 count was included in the test. HIV+ participants were defined as suppressed if HIV copies/ml were <20 (obtained from the pathology report). All participants provided informed consent, either before surgery or after emergency surgery. The study protocol was approved by the University of KwaZulu-Natal Institutional Review Board (approval BE021/13, titled; Lymphoid Tissue Collection for the study of HIV and TB).

Sample processing

Peripheral blood mononuclear cells (PBMCs) were isolated using histopaque 1077 (sigma-Aldrich) and were cryopreserved at -80^{o}C or stained with an antibody panel for flow cytometry experiments. LN samples were processed from fresh tissue after surgery. Tissue were minced and digested with DNase (20ug/ml) and collagenase (0.5 mg/ml). Tissue were rested in a shaking incubator at 37^{o}C for 30 min and then further processed in the GentleMACS dissociator. Digested tissue were strained through a 70 um cell strainer. Lastly, cells from the LN were isolated by Histopaque 1077 (Sigma-Aldrich) density gradient centrifugation. Cells were stained for flow cytometry analysis, further described in the flow cytometry section below.

Flow cytometry

A complete list of conjugated antibodies used with identifier and source information can be found in supplementary material; Table S3. Fresh LN cells, as mentioned above in Sample processing, were surface stained including a near-infrared live/dead cell viability cell staining kit (Invitrogen) at room temperature for 20 min. Cells were stained with fluorochrome-conjugated monoclonal antibodies, following up with the BD Cytofix/crytoperm step (BD Biosciences). Cells were then washed with PBS and acquired using the BD FACS Aria Fusion (BD Biosciences) for 6 hours in 37ºC incubator. Data were analyzed with FlowJo software (version 10.4.2, TreeStar).

Single-cell RNA-seq using Seq-Well v3

After obtaining single-cell suspension from fresh biopsies, we used the Seq-Well platform. Full methods on implementation of this platform is described[42]. Briefly 15,000 cells in 200 uL RPMI + 10% FBS were loaded onto one PDMS array preloaded with barcoded mRNA capture beads (ChemGenes) and settled by gravity into each well. The loaded arrays were washed with PBS and sealed using a semipermeable polycarbonate membrane with a pore size of 0.01 μm, allowing buffers to be exchanged, but retains biological molecules within each nanowell. Arrays were incubated in a dry 37ºC oven for 40 min and further submerged in a lysis buffer a solution containing, guanidium thiocyanate (Sigma), EDTA, 1% beta-mercaptoethanol and sarkosyl (Sigma) for 20 min at RT. Arrays were transferred to hybridization buffer containing NaCl (Fisher Scientific) and supplemented with 8% (v/v) polyethylene glycol (PEG, Sigma) and agitated for 40 min at RT, mRNA capture beads with mRNA hybridized were collected from each Seq-Well array, and beads were resuspended in a master mix for reverse transcription containing Maxima H Minus Reverse Transcriptase (ThermoFisher EP0753) and buffer, dNTPs, RNase inhibitor, a 50 template switch oligonucleotide, and PEG for 30 min at RT, and overnight at 52 ºC with end-over-end rotation. Exonuclease I treatment (New England Biolabs M0293L) to remove excess primers. Following, exonuclease digestion, bead-associated cDNA denatured for 5 min in 0.2 mM NaOH with end over end rotation. Next, beads were washed with TE + 0.01% tween-20, and second strand synthesis was carried out by resuspending beads in a master mix containing Klenow Fragment (NEB), dNTPs, PEG, and the dN-SMRT oligonucleotide to enable random priming off of the beads. PCR amplificationwas performed using KAPA HiFi PCR Mastermix (Kapa Biosystems KK2602) with 2.00 beads per 50 μL reaction volume. Post—whole transcriptome amplification, libraries were then pooled in sets of six (12.000 beads) and purified using Agencourt AMPure XP SPRI beads (Beckman Coulter, A63881) by a 0.6x volume ratio, followed by a 0.8x. Libraries size was

analysed using an Agilent Tapestation hsD5000 kit (Agilent Genomics) with an expected peak at 1000 bp. Libraries were quantified using Qubit High-Sensitivity DNA kit and preparation kit and libraries were constructed using Nextera XT DNA tagmentation (Illumina FC-131-1096) using 800 pg of pooled cDNA library as input using index primers with format as in *Gierahn et al*. Amplified libraries were washed twice with AMpure XP SPRI beads, with a volume ratio of 0.6x followed by 0.8x yielding library sizes with an average distribution of 650-750 pb. Libraries were pooled and sequenced together using a Illumina NovaSeq 6000 S2 Reagent kit v1.5 (100 cycles) using a paired end read structure with custom read 1 primer: read 1: 20 bases with a 12 bases cell barcode and 8 bases unique molecular identifier (UMI). Read 2: 82 bases of transcript information, index 1 and index 2: 8 bases.

Single-cell RNA-seq Computational Pipeline and Analysis

Raw data from the sequence machine was converted to demultiplexed FASTQ files using bcl2fastq2 based on the Nextera N700 indices, which is corresponding to individual arrays. Reads were then aligned to hg19 genome assembly and aligned using the Dropseq-tools pipeline on Terra (app.terra.bio). I analyzed the scRNA-seq data using the *Seurat package*[78]. Data was normalized, scaled and further analysed using Seurat R package v.3.1.0 [82] (https://satijalab.org/seurat/), any cell with fewer than 750 UMIs or greater than 2500 UMIs were excluded. The cell-by-genes matrix was then used to create a Seurat object for further analysis. Cells with any gene expressed in fewer than 5 cells were discarded from downstream analysis and any cell with at least 300 unique genes was retained. Cells with < 5% of UMIs mapping to mitochondrial genes were then removed. These objects were than merged into one object for pre-processing and cell-type identification. The Seurat object was log-normalized to UMI+1 and applying a scale factor of 10.000. Harmony package was used for batch correction. I examined highly variable genes across all cells. I then performed Principal component analysis (PCA) and by using the JackStraw function within Seurat, I identified significant PCs to be used for clustering and further dimensionality reduction. For clustering, I used a Uniform Manifold Approximation and Projection (UMAP) dimensionality reduction technique and with "min dist" set to 0.5 and "n neighbors" set to 30 to identify clusters of transcriptionally similar cells, I employed unsupervised clustering using the FindClusters tool within the Seurat R package with default parameters and k.param set to 10 and resolution set to 0.5. Differential expression analysis between the clusters of were performed using the Seurat package FindAllMarkers in Seurat v3 (setting "test.use" to bimod). For each cluster, differentially DEGs were generated relative to all the other cells. Gene ontology was identified using resource papers[43–45] for marker genes used to identify what clusters were what cell type. DEGs were also generated between ILC3s from HIV negative samples and HIV positive (suppressed). The subset() function in Seurat was used to subset KIT expressing (KIT>1) to isolate ILC3s. In order to subset on

TGFB1 expressing cells, the subset() function was used for ILC3 dataset and the UT dataset (TGFB1>0.001).

Fluorescent immunohistochemistry

Multiplex fluorescent immunohistochemistry experiment was performed using the OpalTM 4-Color Manual IHC kit (PerkinElmer) according to the manufacturer's instructions. Briefly, LN tissue samples fixed with 4% formalin for a minimum of 48 hours were paraffin-embedded. Exactly 4 μm sections were cut, deparaffinized and stained with the following unlabelled primary antibodies: CD117 (clone: ACK2, Abcam), CD3 (clone: Sp7, Abcam), p24 (clone: Kal-1, Dako), CXCR5 (clone: AF488, Abcam), Chymase (ab111239, Abcam) and Collagen 1 (ab34710, Abcam). Opal fluorophore FITC (Opal520) was used for p24, Chymase, Collagen 1 and CXCR5; Texas-Red (Opal570) was used for CD3 and TGFB; then Cy5 (Opal690) was used for CD117 for signal generation in the different IHC experiments performed. DAPI was used as the nuclear counterstain. Images were acquired on a Zeiss Axio Observer Z1 inverted microscope (Olympus) and analyzed with TissueFAXS imaging (TissueGnostics).

References

1. World Health Organization. HIV/AIDS. *https://www.who.int/news-room/fact-sheets/detail/hiv-aids* (2021).
2. Gallo, R. C. *et al.* Isolation of Human T-Cell Leukemia Virus in Acquired Immune Deficiency Syndrome (AIDS). *Science (1979)* **220**, 865–867 (1983).
3. Barré-Sinoussi, F. *et al.* Isolation of a T-Lymphotropic Retrovirus from a Patient at Risk for Acquired Immune Deficiency Syndrome (AIDS). *Science (1979)* **220**, 868–871 (1983).
4. Fettig, J., Swaminathan, M., Murrill, C. S. & Kaplan, J. E. Global Epidemiology of HIV. *Infectious Disease Clinics of North America* **28**, 323–337 (2014).
5. Finzi, D. *et al.* Identification of a Reservoir for HIV-1 in Patients on Highly Active Antiretroviral Therapy. *Science (1979)* **278**, 1295–1300 (1997).
6. Chun, T.-W. *et al.* Presence of an inducible HIV-1 latent reservoir during highly active antiretroviral therapy. *Proceedings of the National Academy of Sciences* **94**, 13193–13197 (1997).
7. Hellmuth, J., Valcour, V. & Spudich, S. CNS reservoirs for HIV: implications for eradication. *Journal of Virus Eradication* **1**, 67–71 (2015).
8. McElrath, M. J. *et al.* Comprehensive Assessment of HIV Target Cells in the Distal Human Gut Suggests Increasing HIV Susceptibility Toward the Anus. *JAIDS Journal of Acquired Immune Deficiency Syndromes* **63**, 263–271 (2013).
9. Politch, J. A. *et al.* Highly active antiretroviral therapy does not completely suppress HIV in semen of sexually active HIV-infected men who have sex with men. *AIDS* **26**, 1535–1543 (2012).
10. Kulpa, D. A. & Chomont, N. HIV persistence in the setting of antiretroviral therapy: when, where and how does HIV hide? *J Virus Erad* **1**, 59–66 (2015).
11. Horiike, M. *et al.* Lymph nodes harbor viral reservoirs that cause rebound of plasma viremia in SIV-infected macaques upon cessation of combined antiretroviral therapy. *Virology* **423**, 107–118 (2012).
12. Embretson, J. *et al.* Massive covert infection of helper T lymphocytes and macrophages by HIV during the incubation period of AIDS. *Nature* **362**, 359–362 (1993).
13. Lorenzo-Redondo, R. *et al.* Persistent HIV-1 replication maintains the tissue reservoir during therapy. *Nature* **530**, 51–56 (2016).
14. Pantaleo, G. *et al.* HIV infection is active and progressive in lymphoid tissue during the clinically latent stage of disease. *Nature* **362**, 355–358 (1993).
15. Rothenberger, M. K. *et al.* Large number of rebounding/founder HIV variants emerge from multifocal infection in lymphatic tissues after treatment interruption. *Proceedings of the National Academy of Sciences* **112**, E1126–E1134 (2015).
16. Lederman, M. M. & Margolis, L. The lymph node in HIV pathogenesis. *Seminars in Immunology* **20**, 187–195 (2008).

17. Gilmore, N. J., Prchal, J. F. & Jothy, S. Persistent generalized lymphadenopathy in homosexual men: clinical, pathological and immunologic characteristics. *Can Med Assoc J* **129**, 960–5 (1983).
18. Tindall, B. *et al.* Characterization of the acute clinical illness associated with human immunodeficiency virus infection. *Arch Intern Med* **148**, 945–9 (1988).
19. Estes, J. D. Pathobiology of HIV/SIV-associated changes in secondary lymphoid tissues. *Immunological Reviews* **254**, 65–77 (2013).
20. Schacker, T. W. *et al.* Collagen deposition in HIV-1 infected lymphatic tissues and T cell homeostasis. *Journal of Clinical Investigation* **110**, 1133–1139 (2002).
21. Sanchez, J. L. *et al.* Lymphoid Fibrosis Occurs in Long-Term Nonprogressors and Persists With Antiretroviral Therapy but May Be Reversible With Curative Interventions. *Journal of Infectious Diseases* **211**, 1068–1075 (2015).
22. Biancotto, A. *et al.* Abnormal activation and cytokine spectra in lymph nodes of people chronically infected with HIV-1. *Blood* **109**, 4272–4279 (2007).
23. Vivier, E. *et al.* Innate Lymphoid Cells: 10 Years On. *Cell* vol. 174 1054–1066 Preprint at https://doi.org/10.1016/j.cell.2018.07.017 (2018).
24. Dudakov, J. A., Hanash, A. M. & van den Brink, M. R. M. Interleukin-22: Immunobiology and Pathology. *Annual Review of Immunology* **33**, 747–785 (2015).
25. Spits, H. & di Santo, J. P. The expanding family of innate lymphoid cells: regulators and effectors of immunity and tissue remodeling. *Nature Immunology* **12**, 21–27 (2011).
26. Spits, H. & Cupedo, T. Innate Lymphoid Cells: Emerging Insights in Development, Lineage Relationships, and Function. *Annual Review of Immunology* **30**, 647–675 (2012).
27. Sonnenberg, G. F., Monticelli, L. A., Elloso, M. M., Fouser, L. A. & Artis, D. CD4+ Lymphoid Tissue-Inducer Cells Promote Innate Immunity in the Gut. *Immunity* **34**, 122–134 (2011).
28. Kløverpris, H. N. *et al.* Innate Lymphoid Cells Are Depleted Irreversibly during Acute HIV-Infection in the Absence of Viral Suppression. *Immunity* **44**, 391–405 (2016).
29. Wang, Y. *et al.* HIV-1-induced cytokines deplete homeostatic innate lymphoid cells and expand TCF7-dependent memory NK cells. *Nature Immunology* **21**, 274–286 (2020).
30. Klatt, N. R. *et al.* Loss of mucosal CD103+ DCs and IL-17+ and IL-22+ lymphocytes is associated with mucosal damage in SIV infection. *Mucosal Immunology* **5**, 646–657 (2012).
31. Xu, H. *et al.* IL-17-producing innate lymphoid cells are restricted to mucosal tissues and are depleted in SIV-infected macaques. *Mucosal Immunology* **5**, 658–669 (2012).
32. Reeves, R. K. *et al.* Gut inflammation and indoleamine deoxygenase inhibit IL-17 production and promote cytotoxic potential in NKp44+ mucosal NK cells during SIV infection. *Blood* **118**, 3321–3330 (2011).
33. Li, H. & Reeves, R. K. Functional perturbation of classical natural killer and innate lymphoid cells in the oral mucosa during SIV infection. *Frontiers in Immunology* **3**, (2013).

34. Xu, H., Wang, X., Lackner, A. A. & Veazey, R. S. Type 3 innate lymphoid cell depletion is mediated by TLRs in lymphoid tissues of simian immunodeficiency virus-infected macaques. *The FASEB Journal* **29**, 5072–5080 (2015).
35. Singh, A. *et al.* Innate Lymphoid Cell Activation and Sustained Depletion in Blood and Tissue of Children Infected with HIV from Birth Despite Antiretroviral Therapy. *Cell Reports* **32**, 108153 (2020).
36. Colonna, M. Innate Lymphoid Cells: Diversity, Plasticity, and Unique Functions in Immunity. *Immunity* **48**, 1104–1117 (2018).
37. Bal, S. M., Golebski, K. & Spits, H. Plasticity of innate lymphoid cell subsets. *Nature Reviews Immunology* vol. 20 552–565 Preprint at https://doi.org/10.1038/s41577-020-0282-9 (2020).
38. Cella, M. *et al.* Subsets of ILC3−ILC1-like cells generate a diversity spectrum of innate lymphoid cells in human mucosal tissues. *Nature Immunology* **20**, 980–991 (2019).
39. Brenchley, J. M. *et al.* Microbial translocation is a cause of systemic immune activation in chronic HIV infection. *Nature Medicine* **12**, 1365–1371 (2006).
40. Zeng, M. *et al.* Cumulative mechanisms of lymphoid tissue fibrosis and T cell depletion in HIV-1 and SIV infections. *Journal of Clinical Investigation* **121**, 998–1008 (2011).
41. Deeks, S. G., Overbaugh, J., Phillips, A. & Buchbinder, S. HIV infection. *Nature Reviews Disease Primers* **1**, 15035 (2015).
42. Gierahn, T. M. *et al.* Seq-Well: Portable, low-cost rna sequencing of single cells at high throughput. *Nature Methods* **14**, 395–398 (2017).
43. Xu, K. *et al.* Single-cell RNA sequencing reveals cell heterogeneity and transcriptome profile of breast cancer lymph node metastasis. *Oncogenesis* **10**, 66 (2021).
44. Mazzurana, L. *et al.* Tissue-specific transcriptional imprinting and heterogeneity in human innate lymphoid cells revealed by full-length single-cell RNA-sequencing. *Cell Research* **31**, 554–568 (2021).
45. Björklund, Å. K. *et al.* The heterogeneity of human CD127+ innate lymphoid cells revealed by single-cell RNA sequencing. *Nature Immunology* **17**, 451–460 (2016).
46. Hamey, F. K. *et al.* Single-cell molecular profiling provides a high-resolution map of basophil and mast cell development. *Allergy* **76**, 1731–1742 (2021).
47. Mazzurana, L. *et al.* Suppression of Aiolos and Ikaros expression by lenalidomide reduces human ILC3−ILC1/NK cell transdifferentiation. *European Journal of Immunology* **49**, 1344–1355 (2019).
48. Trapnell, C. *et al.* The dynamics and regulators of cell fate decisions are revealed by pseudotemporal ordering of single cells. *Nature Biotechnology* **32**, 381–386 (2014).
49. Schubert, M. *et al.* Perturbation-response genes reveal signaling footprints in cancer gene expression. *Nature Communications* **9**, 20 (2018).
50. Seif, F. *et al.* The role of JAK-STAT signaling pathway and its regulators in the fate of T helper cells. *Cell Communication and Signaling* **15**, 23 (2017).

51. Allen, C. D. C. *et al.* Germinal center dark and light zone organization is mediated by CXCR4 and CXCR5. *Nature Immunology* **5**, 943–952 (2004).
52. Krystel-Whittemore, M., Dileepan, K. N. & Wood, J. G. Mast Cell: A Multi-Functional Master Cell. *Frontiers in Immunology* **6**, (2016).
53. Prud'homme, G. J. Pathobiology of transforming growth factor β in cancer, fibrosis and immunologic disease, and therapeutic considerations. *Laboratory Investigation* **87**, 1077–1091 (2007).
54. Batlle, E. & Massagué, J. Transforming Growth Factor-β Signaling in Immunity and Cancer. *Immunity* **50**, 924–940 (2019).
55. Krämer, A., Green, J., Pollard, J. & Tugendreich, S. Causal analysis approaches in Ingenuity Pathway Analysis. *Bioinformatics* **30**, 523–530 (2014).
56. Chatterjee, P., Chiasson, V. L., Bounds, K. R. & Mitchell, B. M. Regulation of the Anti-Inflammatory Cytokines Interleukin-4 and Interleukin-10 during Pregnancy. *Frontiers in Immunology* **5**, (2014).
57. GeneCards. NFE2L2 Gene - NFE2 Like BZIP Transcription Factor 2. *https://www.genecards.org/cgi-bin/carddisp.pl?gene=NFE2L2* (2022).
58. Dimopoulos, Y., Moysi, E. & Petrovas, C. The Lymph Node in HIV Pathogenesis. *Current HIV/AIDS Reports* **14**, 133–140 (2017).
59. Shah, S. v., Manickam, C., Ram, D. R. & Reeves, R. K. Innate lymphoid cells in HIV/SIV infections. *Frontiers in Immunology* vol. 8 Preprint at https://doi.org/10.3389/fimmu.2017.01818 (2017).
60. Arthurs, C. *et al.* Expression of ribosomal proteins in normal and cancerous human prostate tissue. *PLOS ONE* **12**, e0186047 (2017).
61. le Breton, L. & Mayer, M. P. A model for handling cell stress. *Elife* **5**, (2016).
62. Fuchs, A. *et al.* Intraepithelial Type 1 Innate Lymphoid Cells Are a Unique Subset of IL-12- and IL-15-Responsive IFN-γ-Producing Cells. *Immunity* **38**, 769–781 (2013).
63. Li, J. *et al.* Enrichment of IL-17A+IFN-γ+ and IL-22+IFN-γ+ T cell subsets is associated with reduction of NKp44+ILC3s in the terminal ileum of Crohn's disease patients. *Clinical and Experimental Immunology* **190**, 143–153 (2017).
64. Takayama, T. *et al.* Imbalance of NKp44+NKp46− and NKp44−NKp46+ Natural Killer Cells in the Intestinal Mucosa of Patients With Crohn's Disease. *Gastroenterology* **139**, 882-892.e3 (2010).
65. Spits, H., Bernink, J. H. & Lanier, L. NK cells and type 1 innate lymphoid cells: Partners in host defense. *Nature Immunology* vol. 17 758–764 Preprint at https://doi.org/10.1038/ni.3482 (2016).
66. Bernink, J. H. *et al.* Interleukin-12 and -23 Control Plasticity of CD127+ Group 1 and Group 3 Innate Lymphoid Cells in the Intestinal Lamina Propria. *Immunity* **43**, 146–160 (2015).
67. Fuchs, A. & Colonna, M. Innate lymphoid cells in homeostasis, infection, chronic inflammation and tumors of the gastrointestinal tract. *Current Opinion in Gastroenterology* **29**, 581–587 (2013).

68. Bernink, J. H. *et al.* Human type 1 innate lymphoid cells accumulate in inflamed mucosal tissues. *Nature Immunology* **14**, 221–229 (2013).
69. Forkel, M. & Mjösberg, J. Dysregulation of Group 3 Innate Lymphoid Cells in the Pathogenesis of Inflammatory Bowel Disease. *Current Allergy and Asthma Reports* **16**, 73 (2016).
70. Buonocore, S. *et al.* Innate lymphoid cells drive interleukin-23-dependent innate intestinal pathology. *Nature* **464**, 1371–1375 (2010).
71. Evans, T. I. *et al.* SIV-induced Translocation of Bacterial Products in the Liver Mobilizes Myeloid Dendritic and Natural Killer Cells Associated With Liver Damage. *Journal of Infectious Diseases* **213**, 361–369 (2016).
72. Estes, J. D. *et al.* Damaged Intestinal Epithelial Integrity Linked to Microbial Translocation in Pathogenic Simian Immunodeficiency Virus Infections. *PLoS Pathogens* **6**, e1001052 (2010).
73. Takeda, K., Kaisho, T. & Akira, S. Toll-Like Receptors. *Annual Review of Immunology* **21**, 335–376 (2003).
74. Sanjabi, S., Zenewicz, L. A., Kamanaka, M. & Flavell, R. A. Anti-inflammatory and pro-inflammatory roles of TGF-β, IL-10, and IL-22 in immunity and autoimmunity. *Current Opinion in Pharmacology* **9**, 447–453 (2009).
75. Muro-Cacho, C. A., Pantaleo, G. & Fauci, A. S. Analysis of apoptosis in lymph nodes of HIV-infected persons. Intensity of apoptosis correlates with the general state of activation of the lymphoid tissue and not with stage of disease or viral burden. *J Immunol* **154**, 5555–66 (1995).
76. Presicce, P., Shaw, J. M., Miller, C. J., Shacklett, B. L. & Chougnet, C. A. Myeloid dendritic cells isolated from tissues of SIV-infected Rhesus macaques promote the induction of regulatory T cells. *AIDS* **26**, 263–273 (2012).
77. Ipp, H. & Zemlin, A. The paradox of the immune response in HIV infection: When inflammation becomes harmful. *Clinica Chimica Acta* **416**, 96–99 (2013).
78. Stuart, T. *et al.* Comprehensive Integration of Single-Cell Data. *Cell* **177**, 1888-1902.e21 (2019).

Supplementary material

Table S1: Clinical parameters of formalin-fixed paraffin-embedded lymph nodes

PID	Participant	Lymph node Type	Age	Sex	Race	HIV status	Currently on ARTs	ART medication	Reason for procedure	Global Viral Load (cps/mL)	Global CD4 count (cells/μL)
022-09-5025	D	Not specified	38	Female	Indian	Positive	Yes	OAT	Jejunostomy	<20	741
022-09-5044	C	General Lymph Node	61	Female	Black	Positive	Unk	Unk	Cancer	<20	375
022-09-5069	H	Mesenteric	44	Male	Black	Positive	Yes	OAT	Routine surgery	<20	737
022-09-5005	A	Not specified	62	Female	Black	Negative	N/A	N/A	Cancer	N/A	N/A
022-09-5009	F	Mesenteric	47	Female	Black	Negative	N/A	N/A	Routine surgery	N/A	N/A
022-09-5062	B	Common hepatic	47	Female	Black	Negative	N/A	N/A	Routine surgery	N/A	N/A
022-09-5088	E	Not specified	55	Female	Black	Negative	N/A	N/A	Routine surgery	N/A	N/A
022-09-5065	G	General Lymph Node	37	Female	Black	Positive	Yes	OAT	Routine surgery	27	209

N/A, not available
PID, participant identification number
Unk, unknown
All participants had no TB history, except 022-09-5069
OAT, Odimune/Atrioza/Tribuss

Table S2: Clinical parameters of single-cell RNA-seq dataset (without sorting, TGFB1_UT)

PID	Lymph node Type	Age (years)	Sex	Race	HIV status	Currently on ARTs	ART Medication	Reason for Procedure	Global Viral Load (cps/mL)	Global CD4 count (cells/μL)
022-09-5025	Mesenteric	38	Female	Indian	Positive	Yes	OAT	Jejunostomy	<20	741
022-09-5046	Cystic Duct	Unk	Male	Unknown	Positive	Unk	Unk	Unknown	<20	752
022-09-5056	Common Hepatic	18	Male	Black	Positive	Unk	Unk	Adrenalectomy	<20	800
022-09-5007	Mesenteric	39	Female	Black	Positive	Yes	OAT	Cyst	<20	Unknown
022-09-5029	Celiac	49	Female	Indian	Positive	Yes	OAT	Pancreatectomy	<20	784
022-09-5044	Mesenteric	61	Female	Black	Positive	Unk	Unk	Cancer	<20	375
022-09-5062	Hepatic	47	Female	Black	Negative	N/A	N/A	Routine surgery	N/A	N/A
022-09-5058	Celiac	23	Female	Black	Negative	N/A	N/A	Routine surgery	N/A	N/A
022-09-5059	Bile	36	Female	Black	Negative	N/A	N/A	Routine surgery	N/A	N/A
022-09-5061	Common Hepatic	55	Male	Indian	Negative	N/A	N/A	Routine surgery	N/A	N/A

N/A, not available
PID, participant identification number
Unk, unknown
All participants had no TB history, except 022-09-5029
OAT, Odimune/Atrioza/Tribuss

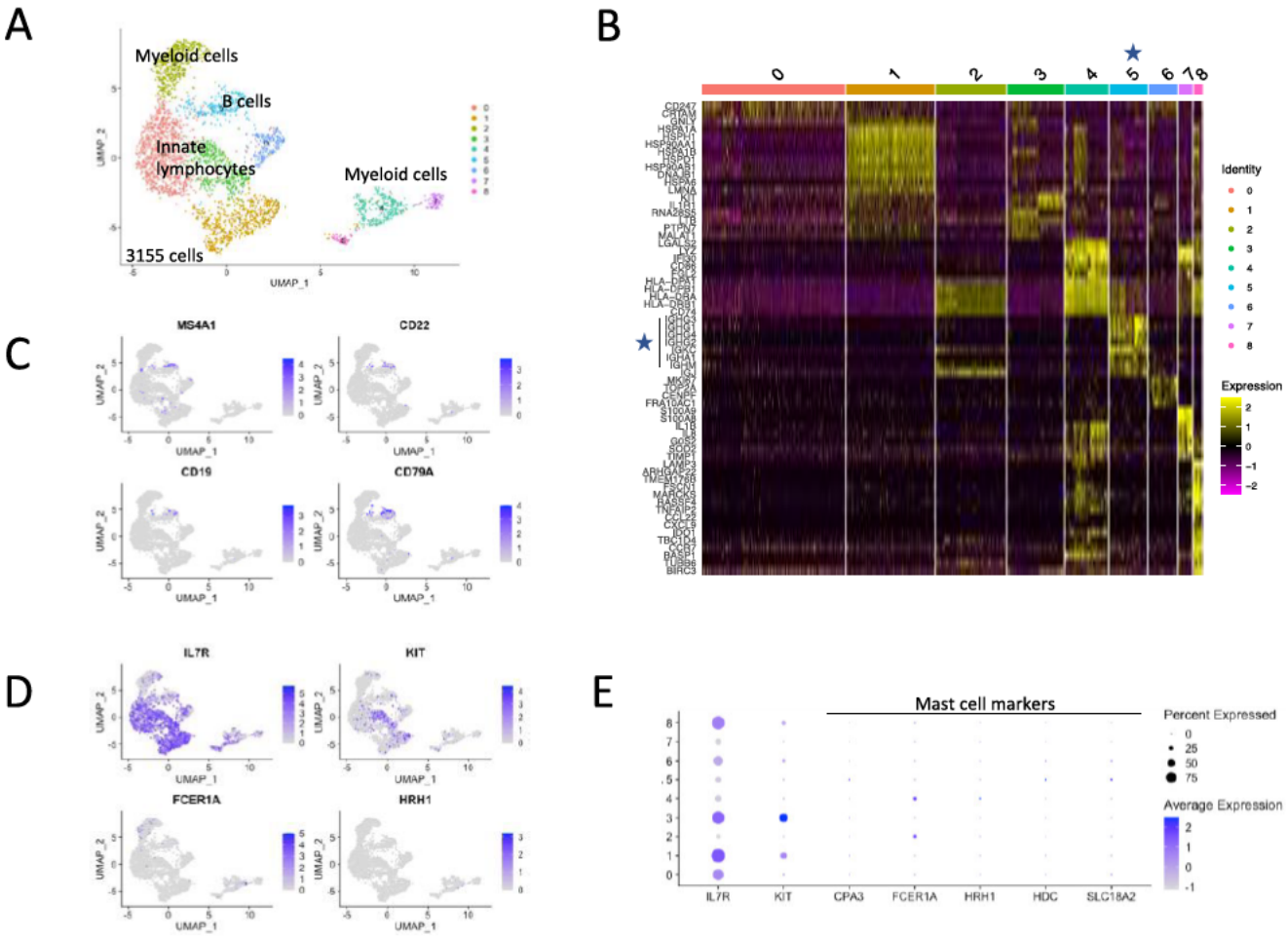

Figure S1. Identifying B-cells for exclusion from dataset. A) UMAP projection of all cells coloured by cluster. B) HeatMap depicting top 10 differentially expressed genes between clusters. C) FeaturePlot highlighting B-cell marker transcripts. D) FeaturePlot highlighting markers of ILC3s (IL7R, KIT) and Mast cells (FCER1A, HRH1). E) DotPlot highlighting Mast cell marker transcripts in the various clusters.

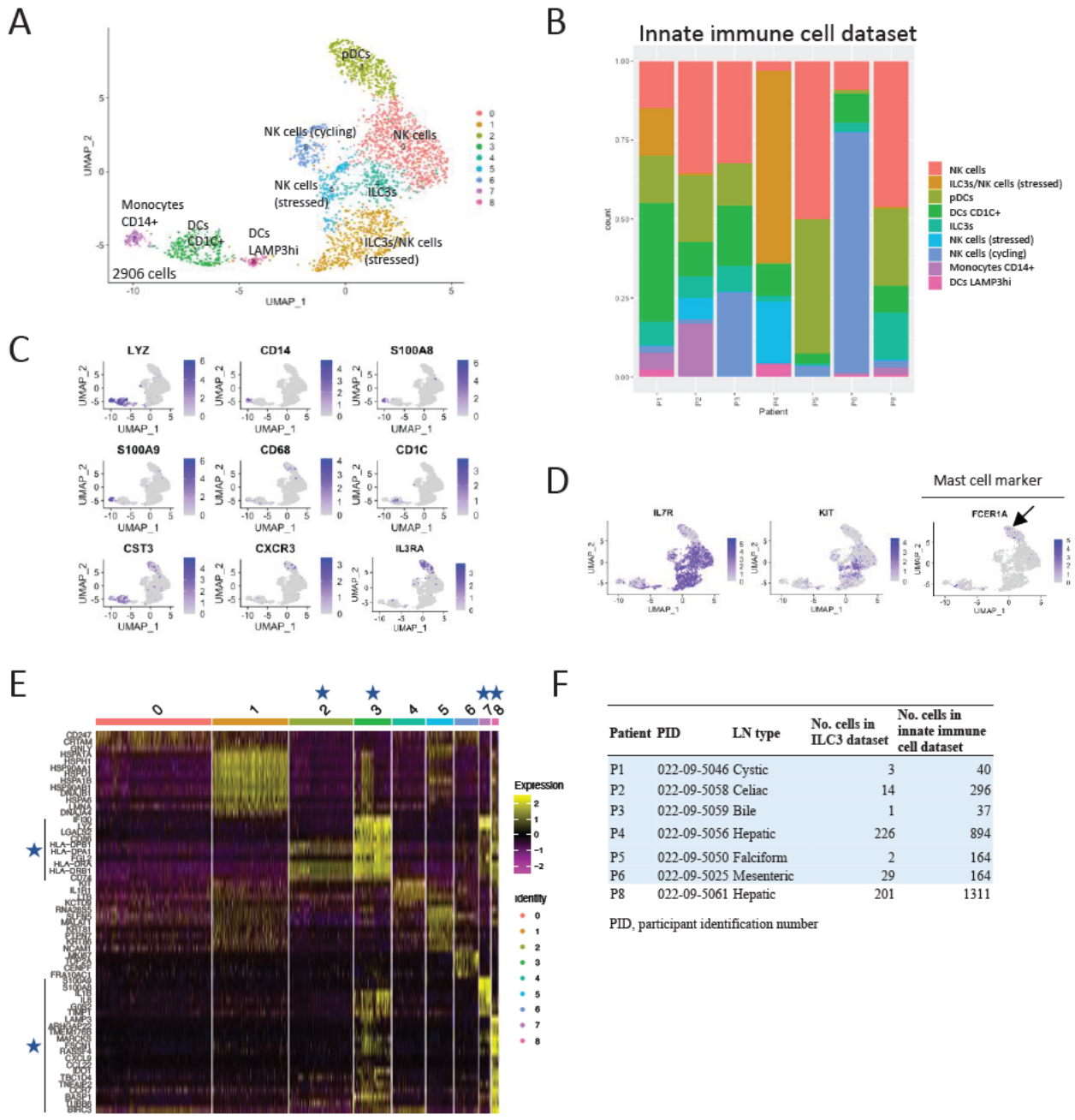

Patient	PID	LN type	No. cells in ILC3 dataset	No. cells in innate immune cell dataset
P1	022-09-5046	Cystic	3	40
P2	022-09-5058	Celiac	14	296
P3	022-09-5059	Bile	1	37
P4	022-09-5056	Hepatic	226	894
P5	022-09-5050	Falciform	2	164
P6	022-09-5025	Mesenteric	29	164
P8	022-09-5061	Hepatic	201	1311

PID, participant identification number

Figure S2. Innate immune cell dataset. A) UMAP projection of different cellular clusters. B) Cellular composition between participants. C) FeaturePlot of myeloid cell marker transcripts. D) FeaturePlot of ILC3 markers (IL7R, KIT) and a Mast cell marker transcript (FCER1A). E) HeatMap of differentially expressed genes between clusters. The stars highlight myeloid clusters and their respective DEGs. F) Number of cells from each participant in either the ILC3 dataset or the innate immune cell dataset.

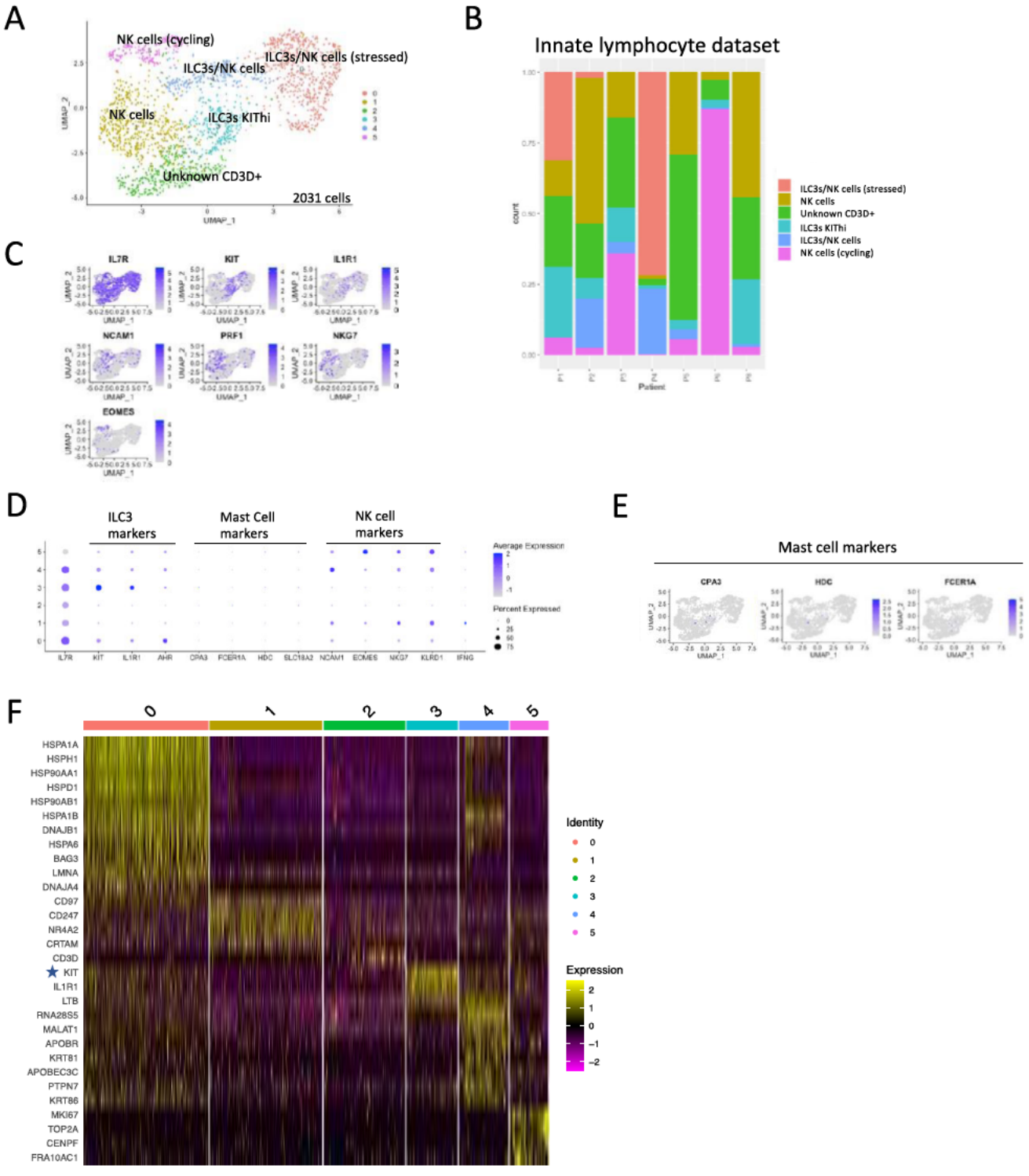

Figure S3. Innate lymphocyte dataset. A) UMAP projection of the different cellular clusters. B) Cellular composition between participants. C) FeaturePlot of ILC3 marker transcripts (IL7R, KIT, IL1R1) and NK cell marker transcripts (NCAM1, PRF1, NKG7, EOMES). D) DotPlot of canonical ILC3, Mast cell and NK cell transcripts. E) FeaturePlot of Mast cell markers. F) HeatMap of top 10 differentially expressed genes between clusters.

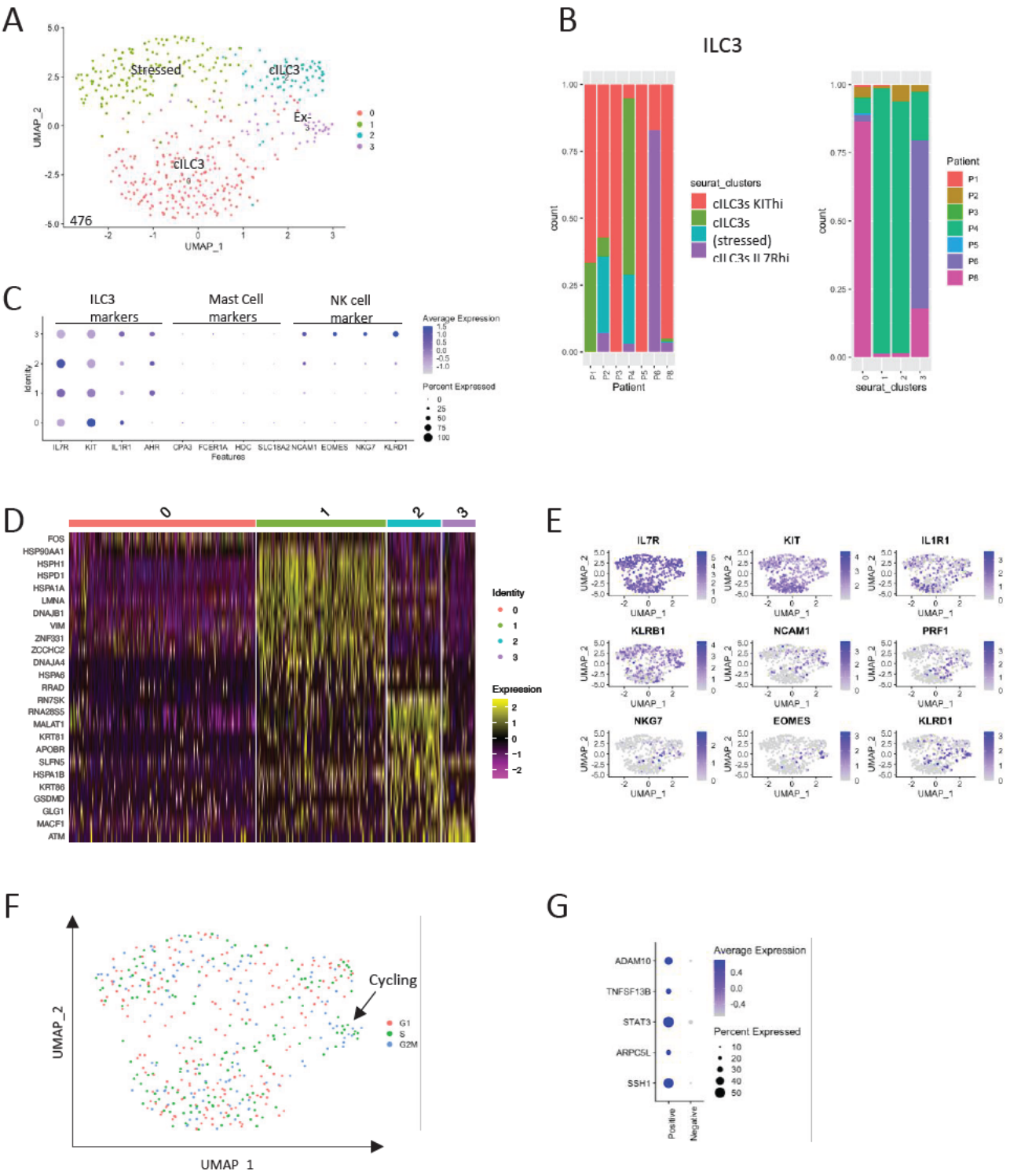

Figure S4. ILC3 dataset. A) UMAP projection of the different cellular clusters. B) Cellular composition between participants. C) DotPlot of canonical ILC3, Mast cell and NK cell transcripts. D) HeatMap of top 10 differentially expressed genes between clusters. E) FeaturePlot of ILC3 marker (IL7R, KIT, IL1R1) and NK marker (NCAM1, PRF1, NKG7, EOMES, KLRD1) transcripts. F) UMAP projection highlighting cell cycle. G) DotPlot showing transcripts of interest between disease states.

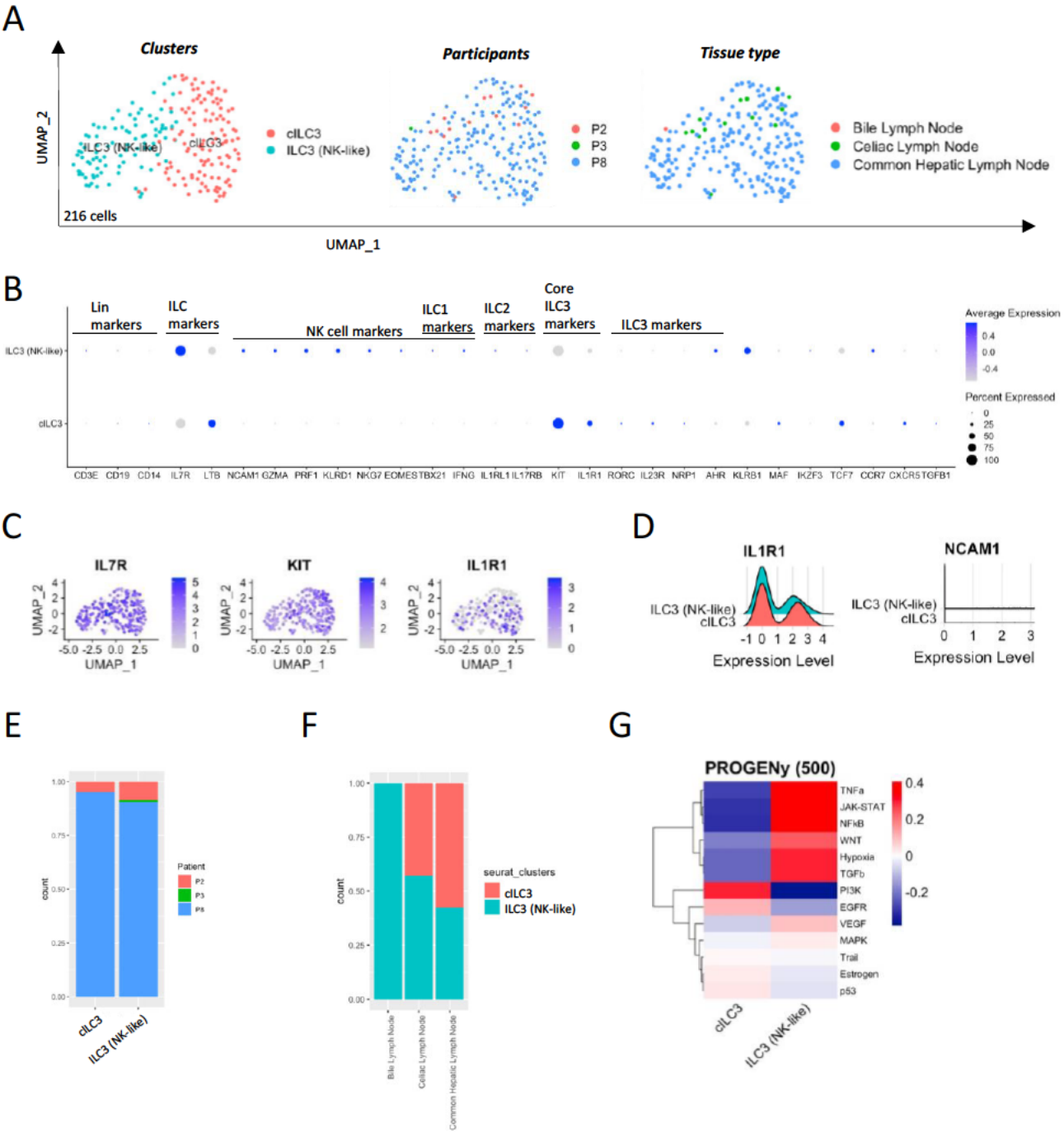

Figure S5. Characterizing ILC3s from HIV negative LNs. A) UMAP projections highlighting cluster, participant and tissue type. B) DotPlot charactering the ILC3 clusters with canonical ILC marker transcripts, including transcripts of interest. C) FeaturePlot of canonical ILC3 marker transcripts. D) RidgePlot highlighting IL1R1 and NCAM1 expression between clusters. E) Cells per participant composition per cluster. F) Cells per cluster per tissue type. G) *PROGENy* analysis per cluster.

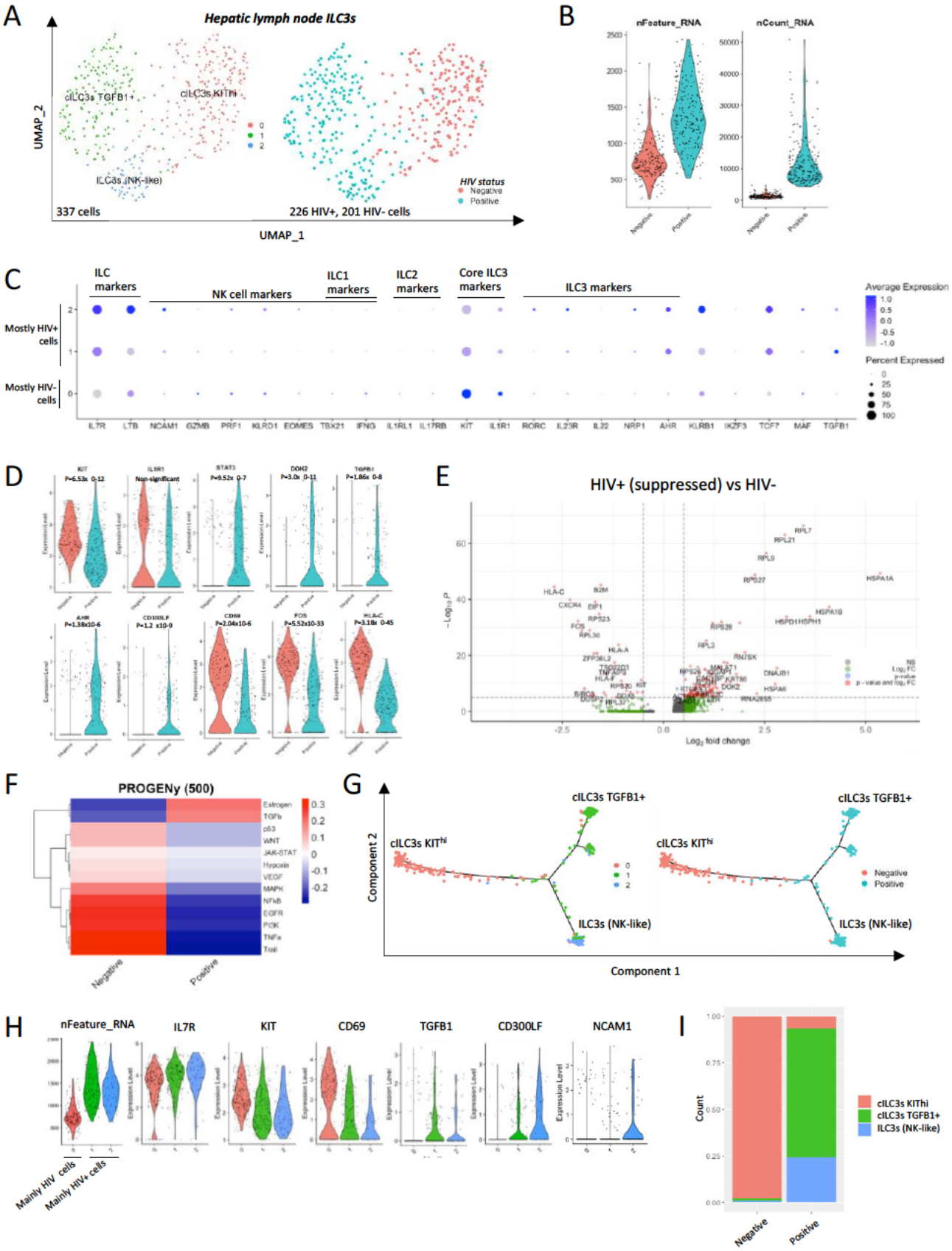

Figure S6. The impact of HIV on ILC3s from two common hepatic lymph nodes. A) UMAP projections of the common hepatic ILC3 datasets, highlighting clusters and disease state. B) ViolinPlots

comparing total gene expression (nFeature_RNA) and transcript expression (nCount_RNA) between disease states. C) A DotPlot charactering the ILC3 clusters with canonical ILC marker transcripts, including transcripts of interest. D) ViolinPlots comparing expression levels of various genes. E) VolcanoPlot representing differentially expressed genes from HIV positive (suppressed) ILC3s compared to HIV negative ILC3s, from common hepatic lymph nodes. F) A *PROGENy* analysis comparing signaling pathways from common hepatic ILC3s between disease states. G) Trajectory analyses of the common hepatic lymph node dataset, highlighting clusters and disease state. H) ViolinPlots highlighting the total amount of genes transcribed (nFeature_RNA), RNA transcribed (nCount_RNA), and expression level of genes of interest, compared between clusters. I) Comparing cellular composition between disease states.

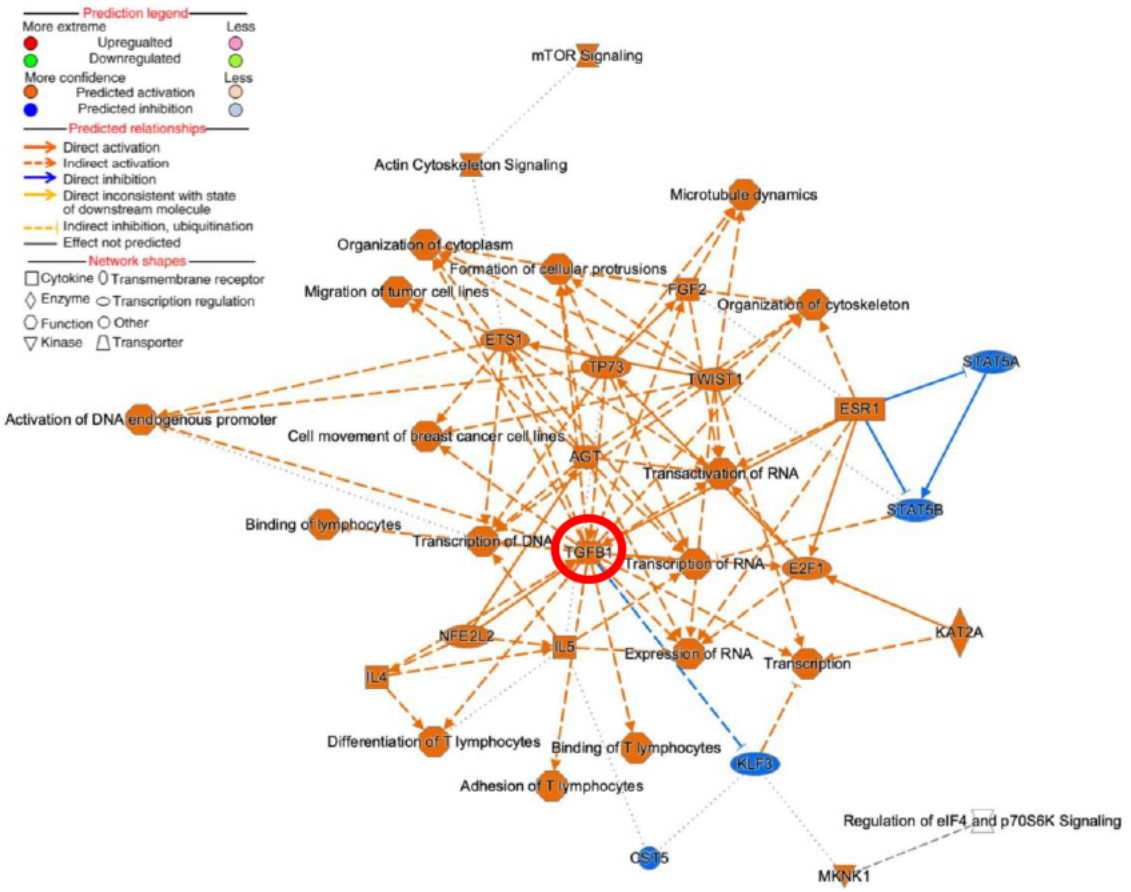

Figure S7. Graphical summary obtained using IPA. DEGs from ILC3s in LNs between disease states. Q-value set to 0.12 cutoff.

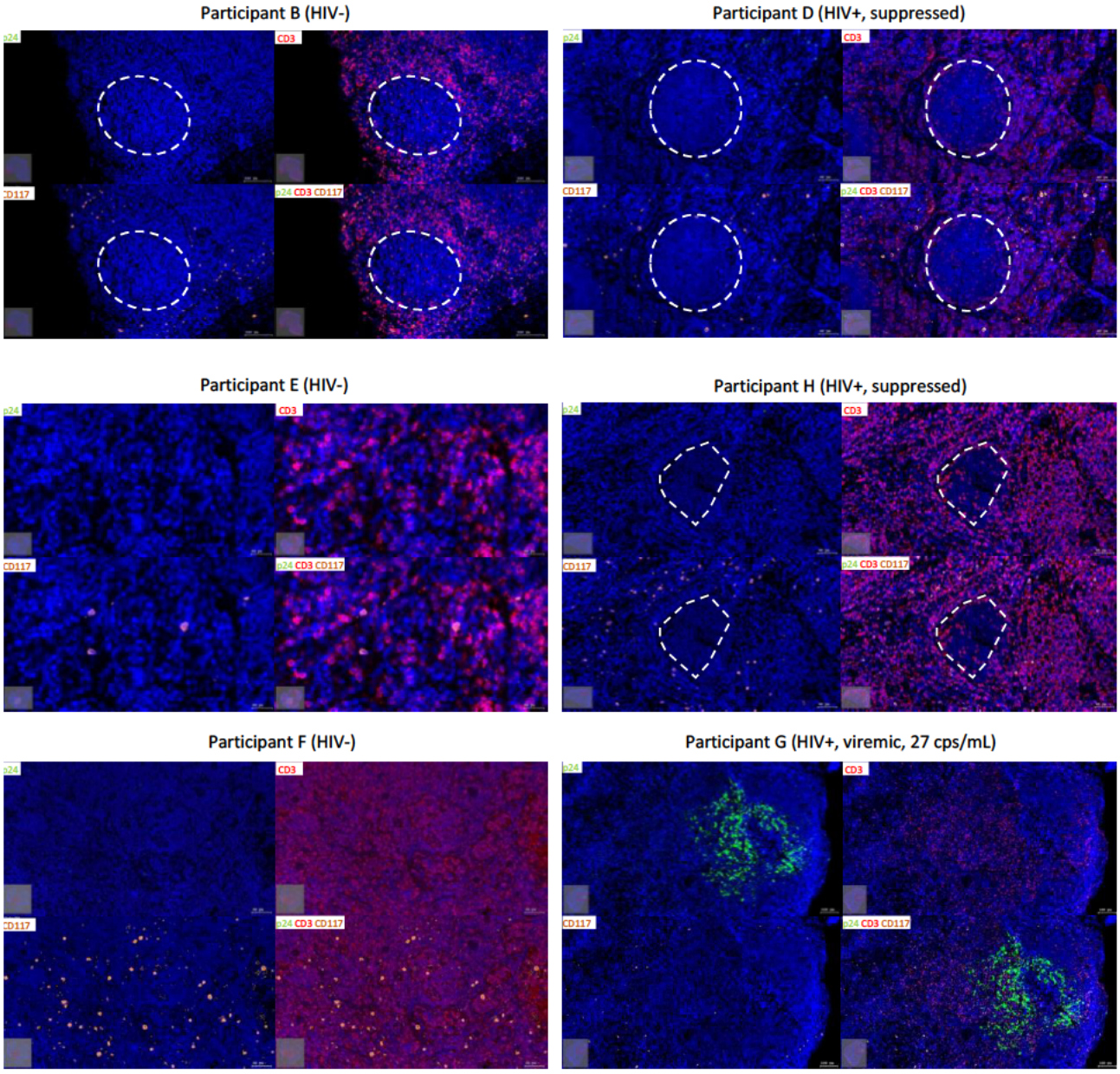

Figure S8. F-IHC of FFPE lymph nodes, stained with p24 (HIV antigen), CD3 (T-cell antigen) and CD117. Participants E, F and G did not have definitive germinal centers. Scale bars in bottom right corner of each image.

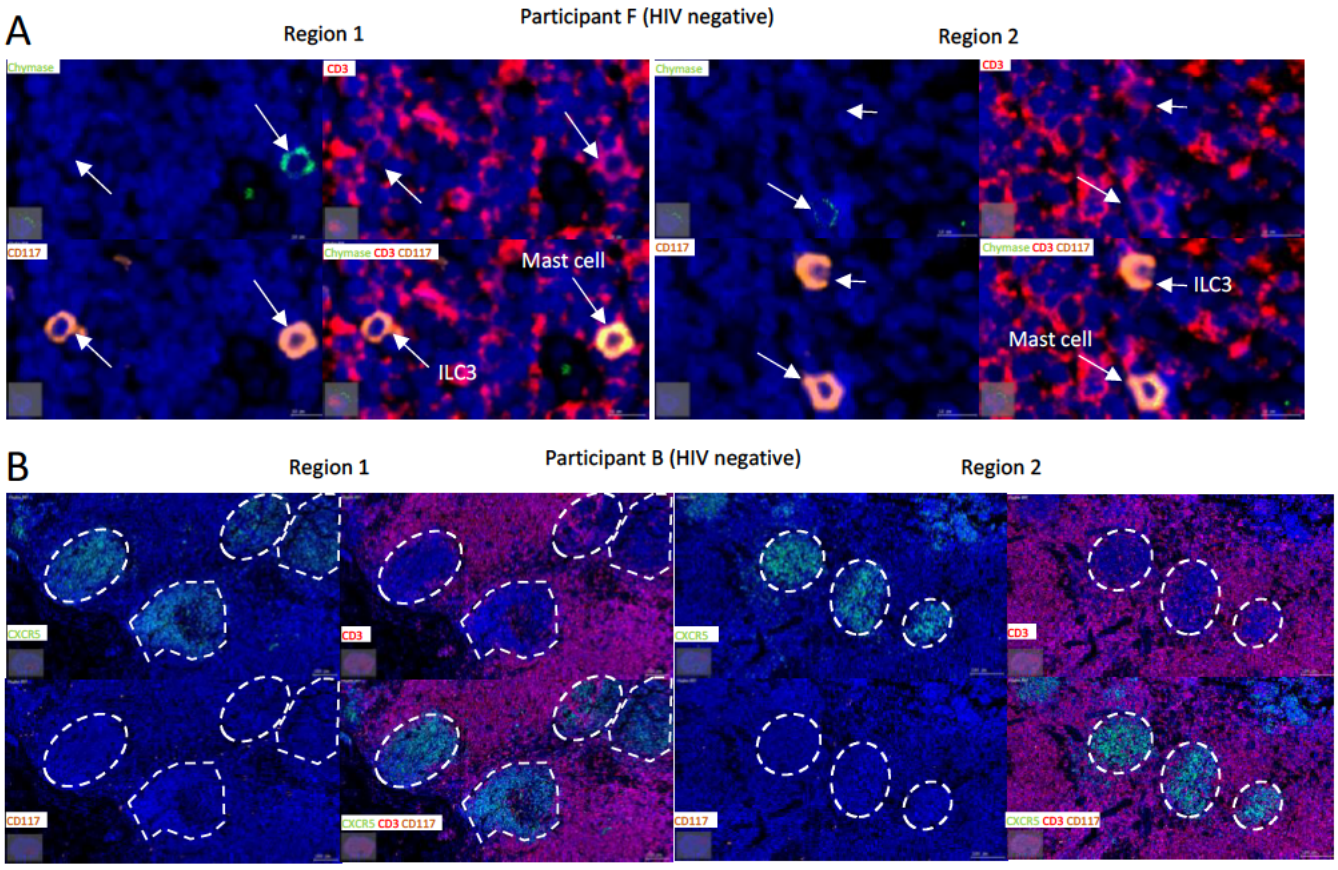

Figure S9. F-IHC control and GC identification images. A) HIV- lymph node stained with Chymase (Mast cell marker), CD3 and CD117. This identifies a Mast cell (Chymase+CD117+) and an ILC3 (Chymase-CD117+) in both region 1 and 2. B) Further germinal center identification in an HIV- lymph node. GCs are outlined with a dashed line. Scale bars in bottom right corner.

Table S3: Conjugated antibodies used to sort CD3-CD19- cells

Conjugated antibodies	**Source**	**Catalogue number**
Anti-CD94 FITC	BD Bioscience	555888
Anti-CD117 BV650	BioLegend	313221
Anti-CD19 BV605	BioLegend	302244
Anti-CD161 BV605	BioLegend	302041
Anti-CD56 BV711	BioLegend	318336
Anti-CD69 BV785	BioLegend	310932
Anti-CD4 AF700	BioLegend	100430
Anti-CD19 PE	BioLegend	302254
Anti-CD127 Pe-Cy7	Beckman Coulter	PNA64618
Anti-CRTH2 APC	BioLegend	350110
Anti-CD103 BV421	BD Biosciences	562771
Anti-CD69 BV785	BioLegend	310932
Anti-CD3 PE-CF594	BD Biosciences	562280
Anti-CD8 BUV395	BioLegend	563794
Anti-CD366 (NKp44) PE-Cy5	Beckman Coulter	A66903
Anti-CD16 BUV496	BioLegend	612944
Anti-CD45 V500	BioLegend	560779
Live/Dead Fixable	Invitrogen	L10119

CHAPTER 3: DISCUSSION/SYNTHESIS

LNs play a key role in the immune system since their structure provides the support for a multitude of complex intercellular interactions involved in building an immune response to an invading pathogen[19]. A major pathological consequence of HIV is sustained inflammation and fibrosis in LNs which leads to LNs becoming dysfunctional and therefore leads to an impaired immune response[19], which contributes to the progression of AIDS. ILCs are innate immune cells which are mainly tissue resident and therefore are one of the first responders to infection[20]. The function of ILCs in LNs is unclear as well as their relationship with HIV in LNs. In this dissertation, I aimed to (1) investigate the impact of HIV infection on ILC3s in LNs from treated and virally suppressed PLWH. I also sort to test the hypotheses; (i) ILC3s participate in the immune response during HIV infection and (ii) HIV infection leads to ILC3s transdifferentiating into ex-ILC3s, driven by the highly proinflammatory tissue microenvironment in LNs.

From my results (graphical summary in Figure 1), I found that ILC3s seem to become activated during HIV infection and that ILC3s also upregulated functional cytokines known to participate in immune responses, such as TGFβ and GZMA. These, along with other findings, such as the emergence of cytotoxic 'ex-ILC3s', led me to conclude that ILC3s probably participate in an immune response towards HIV infection, which may be to participate in a type 1 immune response, however, their exact role remains unclear. Therefore, to fully confirm my first hypothesis, studies investigating functionality are warranted, such as *in vitro* LN-resident ILC3 stimulation assays with inflammatory cytokines or HIV peptides.

While investigating my second hypothesis, I found that HIV infection led to the emergence of an ex-ILC3 population which had cytotoxic potential. Previous studies have hypothesized that ex-ILC3s transdifferentiate from conventional ILC3s due to an inflamed tissue microenvironment. I found that HIV infection led to a distinct ex-ILC3 population, however, an NK-like ILC3 population was also detected in HIV negative LNs. The NK-like ILC3s did not have any DEGs compared to the cILC3 population in HIV negative LNs, hinting that these two populations may not be terminally differentiated or are quiescent during homeostatic conditions. The NK-like ILC3 population did share some NK cell-associated transcripts with the ex-ILC3 population. This suggests that the ex-ILC3 population observed in my dataset probably did not transdifferentiate from cILC3s, but rather that HIV infection may have led the NK-like ILC3 population to terminally differentiate into ex-ILC3s. However, to determine what populations during homeostatic conditions terminally differentiate into ex-ILC3s, further experiments must be conducted, such as *in vitro* cell stimulation assays. I hypothesize that HIV-infection, which leads to a highly inflamed LN microenvironment, drives this terminal differentiation. Importantly, this

ex-ILC3 population emerged in conjunction with a cILC3 population which may also be terminally differentiated from the cILC3 population observed in HIV negative LNs.

Interestingly, ILC3s may contribute to HIV-induced fibrosis by either directly stimulating fibroblasts to deposit collagen, through TGFβ stimulation, or indirectly by maintaining T-regs, through TGFβ intercellular signaling, which also stimulate fibroblasts to deposit collagen through TGFβ, or both. The actual amount of TGFβ ILC3s may contribute to the overall amount of TGFβ in LNs during HIV infection is unknown and warrants further investigation. However, this is a novel cell type that was previously unknown to contribute to fibrosis. ELISpot experiments may be conducted to compare the number of TGFβ secreting ILC3s from HIV positive and HIV negative LNs or flow cytometry experiments may be conducted to investigate TGFβ secreting ILC3s.

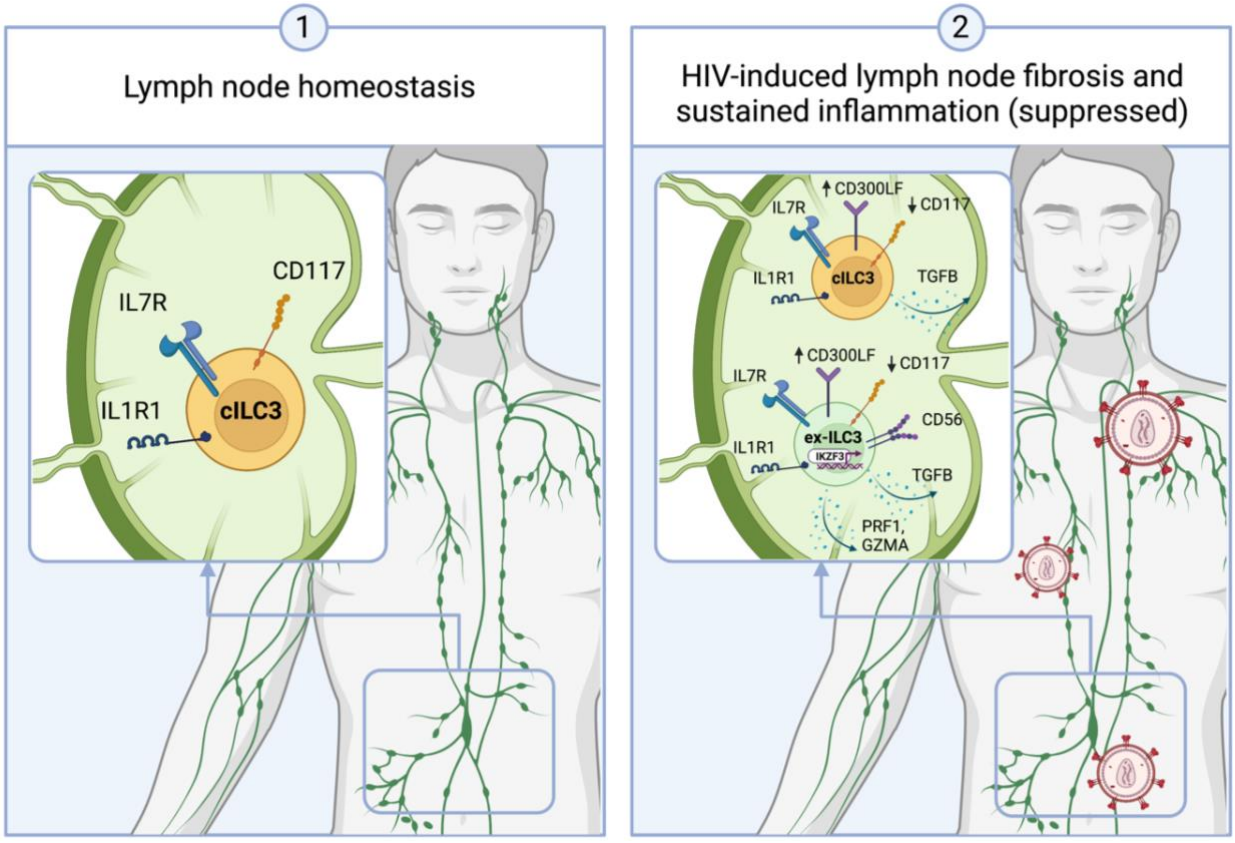

Figure 1. Graphical summary of findings, highlighting prominent ILC3 populations identified between disease states in human LNs. 1) During homeostatic, two ILC3 populations were identified, however, there were no DEGs (adjusted p value) between the two populations. This is probably why only one ILC3 population was observed for HIV negative participants when compared to HIV positive participants, therefore only one population is shown above. 2) Two prominent ILC3 populations were evident during HIV infection. HIV infection leads to a highly inflamed LN microenvironment, which

activates ILC3s which then become terminally differentiated. ILC3s during HIV infection may contribute to fibrosis through the upregulation of TGFβ production which, either directly or indirectly, stimulates fibroblasts to deposit collagen. Also, an 'ex-ILC3' population emerges with cytotoxic potential. Image created using BioRender.com.

There were limitations to the study. There were low sample numbers for scRNA-seq (n=7) which led to low numbers of ILC3 cells in the dataset. More LN samples for scRNA-seq would greatly strengthen the study, not only for more biological replicates and more ILC3s in the dataset, but also to obtain disease states for each tissue type as we did not have an HIV negative mesenteric LN to investigate whether ex-ILC3s are also present during homeostatic conditions in mesenteric LNs. More samples will also allow for age and sex matching, a more thorough investigation into ILC3 plasticity, and a more thorough investigation into the impact of HIV viremia on ILC3s in LNs. However, this is a first-of-its-kind study into characterizing ILCs in LNs *and* investigating the impact of HIV infection, which lays a foundation for further analyses.

I believe that the utilized techniques, namely scRNA-seq and F-IHC, have been adequate in investigating this dissertation's aim and hypotheses. This study may be used as a resource for future studies requiring characterized ILC3s in LNs and the impact of HIV infection on ILC3s in LNs. It is planned that the work done in this dissertation will be submitted for publication which will also include single-cell transcriptional analyses on LN-resident NK cells and myeloid cells, done by myself, and flow cytometry data, from members of the Kløverpris Lab, in a research paper investigating the impact of HIV infection on innate immune cells in LNs. To summarize, I believe I have achieved my aim of investigating the impact of HIV infection on ILC3s in LNs which sets the stage for further characterizing and analyses. My results support my hypotheses, although further analyses are required to determine what population ex-ILC3s differentiate from, and further studies are required to determine to what degree ILC3s participate in HIV-induced fibrosis. Lymphoid tissue fibrosis is a major pathological consequence of HIV infection and contributes to the progression of AIDS. Therefore, identifying cells that may contribute to fibrosis may lead to novel therapeutic techniques aimed at hindering HIV-induced fibrosis thus allowing the preservation of the immune system and subsequent immune responses.

References

1. Merson, M. H., O'Malley, J., Serwadda, D. & Apisuk, C. The history and challenge of HIV prevention. *The Lancet* **372**, 475–488 (2008).
2. Barré-Sinoussi, F. *et al.* Isolation of a T-Lymphotropic Retrovirus from a Patient at Risk for Acquired Immune Deficiency Syndrome (AIDS). *Science (1979)* **220**, 868–871 (1983).
3. Gallo, R. C. *et al.* Isolation of Human T-Cell Leukemia Virus in Acquired Immune Deficiency Syndrome (AIDS). *Science (1979)* **220**, 865–867 (1983).
4. World Health Organization. HIV/AIDS. *https://www.who.int/news-room/fact-sheets/detail/hiv-aids* (2021).
5. UNAIDS. Global HIV & AIDS statistics . *https://www.unaids.org/en/resources/fact-sheet* (2021).
6. UNAIDS. Key Population Atlas. *https://kpatlas.unaids.org/dashboard#/home* (2022).
7. HIV Impact Assessment Summary Report. *THE FIFTH SOUTH AFRICAN NATIONAL HIV PREVALENCE, INCIDENCE, BEHAVIOUR AND COMMUNICATION SURVEY, 2017*. (2018).
8. Dwyer-Lindgren, L. *et al.* Mapping HIV prevalence in sub-Saharan Africa between 2000 and 2017. *Nature* **570**, 189–193 (2019).
9. Fettig, J., Swaminathan, M., Murrill, C. S. & Kaplan, J. E. Global Epidemiology of HIV. *Infectious Disease Clinics of North America* **28**, 323–337 (2014).
10. UNAIDS. Decline in new HIV infections has stalled. *https://www.unaids.org/en/resources/presscentre/featurestories/2021/september/20210913_decline-in-new-hiv-infections-has-stalled* (2021).
11. Clinic Info.HIV.gov. Guidelines for the Use of Antiretroviral Agents in Adults and Adolescents Living with HIV. *https://clinicalinfo.hiv.gov/en/guidelines/adult-and-adolescent-arv/adverse-effects-antiretroviral-agents* (2021).
12. Finzi, D. *et al.* Identification of a Reservoir for HIV-1 in Patients on Highly Active Antiretroviral Therapy. *Science (1979)* **278**, 1295–1300 (1997).
13. Chun, T.-W. *et al.* Presence of an inducible HIV-1 latent reservoir during highly active antiretroviral therapy. *Proceedings of the National Academy of Sciences* **94**, 13193–13197 (1997).
14. Hellmuth, J., Valcour, V. & Spudich, S. CNS reservoirs for HIV: implications for eradication. *Journal of Virus Eradication* **1**, 67–71 (2015).
15. McElrath, M. J. *et al.* Comprehensive Assessment of HIV Target Cells in the Distal Human Gut Suggests Increasing HIV Susceptibility Toward the Anus. *JAIDS Journal of Acquired Immune Deficiency Syndromes* **63**, 263–271 (2013).
16. Politch, J. A. *et al.* Highly active antiretroviral therapy does not completely suppress HIV in semen of sexually active HIV-infected men who have sex with men. *AIDS* **26**, 1535–1543 (2012).
17. Kulpa, D. A. & Chomont, N. HIV persistence in the setting of antiretroviral therapy: when, where and how does HIV hide? *J Virus Erad* **1**, 59–66 (2015).

18. Horiike, M. *et al.* Lymph nodes harbor viral reservoirs that cause rebound of plasma viremia in SIV-infected macaques upon cessation of combined antiretroviral therapy. *Virology* **423**, 107–118 (2012).
19. Lederman, M. M. & Margolis, L. The lymph node in HIV pathogenesis. *Seminars in Immunology* **20**, 187–195 (2008).
20. Vivier, E. *et al.* Innate Lymphoid Cells: 10 Years On. *Cell* vol. 174 1054–1066 (2018).
21. Ebbo, M., Crinier, A., Vély, F. & Vivier, E. Innate lymphoid cells: major players in inflammatory diseases. *Nature Reviews Immunology* **17**, 665–678 (2017).
22. Robinette, M. L. *et al.* Transcriptional programs define molecular characteristics of innate lymphoid cell classes and subsets. *Nature Immunology* **16**, 306–317 (2015).
23. van de Pavert, S. A. Lymphoid Tissue inducer (LTi) cell ontogeny and functioning in embryo and adult. *Biomedical Journal* **44**, 123–132 (2021).
24. Shah, S. v., Manickam, C., Ram, D. R. & Reeves, R. K. Innate lymphoid cells in HIV/SIV infections. *Frontiers in Immunology* vol. 8 (2017).
25. Dudakov, J. A., Hanash, A. M. & van den Brink, M. R. M. Interleukin-22: Immunobiology and Pathology. *Annual Review of Immunology* **33**, 747–785 (2015).
26. Spits, H. & di Santo, J. P. The expanding family of innate lymphoid cells: regulators and effectors of immunity and tissue remodeling. *Nature Immunology* **12**, 21–27 (2011).
27. Spits, H. & Cupedo, T. Innate Lymphoid Cells: Emerging Insights in Development, Lineage Relationships, and Function. *Annual Review of Immunology* **30**, 647–675 (2012).
28. Sonnenberg, G. F., Monticelli, L. A., Elloso, M. M., Fouser, L. A. & Artis, D. CD4+ Lymphoid Tissue-Inducer Cells Promote Innate Immunity in the Gut. *Immunity* **34**, 122–134 (2011).
29. Klatt, N. R. *et al.* Loss of mucosal CD103+ DCs and IL-17+ and IL-22+ lymphocytes is associated with mucosal damage in SIV infection. *Mucosal Immunology* **5**, 646–657 (2012).
30. Xu, H. *et al.* IL-17-producing innate lymphoid cells are restricted to mucosal tissues and are depleted in SIV-infected macaques. *Mucosal Immunology* **5**, 658–669 (2012).
31. Reeves, R. K. *et al.* Gut inflammation and indoleamine deoxygenase inhibit IL-17 production and promote cytotoxic potential in NKp44+ mucosal NK cells during SIV infection. *Blood* **118**, 3321–3330 (2011).
32. Li, H. & Reeves, R. K. Functional perturbation of classical natural killer and innate lymphoid cells in the oral mucosa during SIV infection. *Frontiers in Immunology* **3**, (2013).
33. Xu, H., Wang, X., Lackner, A. A. & Veazey, R. S. Type 3 innate lymphoid cell depletion is mediated by TLRs in lymphoid tissues of simian immunodeficiency virus-infected macaques. *The FASEB Journal* **29**, 5072–5080 (2015).
34. Belz, G. T. ILC2s masquerade as ILC1s to drive chronic disease. *Nature Immunology* **17**, 611–612 (2016).
35. Kløverpris, H. N. *et al.* Innate Lymphoid Cells Are Depleted Irreversibly during Acute HIV-Infection in the Absence of Viral Suppression. *Immunity* **44**, 391–405 (2016).

36. Singh, A. *et al.* Innate Lymphoid Cell Activation and Sustained Depletion in Blood and Tissue of Children Infected with HIV from Birth Despite Antiretroviral Therapy. *Cell Reports* **32**, 108153 (2020).
37. DuPage, M. & Bluestone, J. A. Harnessing the plasticity of CD4+ T cells to treat immune-mediated disease. *Nature Reviews Immunology* **16**, 149–163 (2016).
38. Bal, S. M., Golebski, K. & Spits, H. Plasticity of innate lymphoid cell subsets. *Nature Reviews Immunology* vol. 20 552–565 (2020).
39. Bernink, J. H. *et al.* Interleukin-12 and -23 Control Plasticity of CD127+ Group 1 and Group 3 Innate Lymphoid Cells in the Intestinal Lamina Propria. *Immunity* **43**, 146–160 (2015).
40. Schacker, T. W. *et al.* Collagen deposition in HIV-1 infected lymphatic tissues and T cell homeostasis. *Journal of Clinical Investigation* **110**, 1133–1139 (2002).
41. Gierahn, T. M. *et al.* Seq-Well: Portable, low-cost rna sequencing of single cells at high throughput. *Nature Methods* **14**, 395–398 (2017).

ANNEX

Ethics certificate

UNIVERSITY OF KWAZULU-NATAL
INYUVESI YAKWAZULU-NATALI

07 April 2022

Mr Nicholas Graeme Herbert (221116421)
School of Lab Med & Medical Sc
Medical School

Dear Mr Herbert,

Protocol reference number: BREC/00003988/2022
Project title: Lymphoid Tissue Collection for the study of HIV and TB.
Degree: MMedSc

EXPEDITED APPLICATION: APPROVAL LETTER

A sub-committee of the Biomedical Research Ethics Committee has considered and noted your application.

The conditions have been met and the study is given full ethics approval and may begin as from 07 April 2022. Please ensure that any outstanding site permissions are obtained and forwarded to BREC for approval before commencing research at a site.

This approval is subject to national and UKZN lockdown regulations, see (http://research.ukzn.ac.za/Libraries/BREC/BREC_Amended_Lockdown_Level_1_Guidelines.sflb.ashx). Based on feedback from some sites, we urge PIs to show sensitivity and exercise appropriate consideration at sites where personnel and service users appear stressed or overloaded.

This approval is valid for one year from 07 April 2022. To ensure uninterrupted approval of this study beyond the approval expiry date, an application for recertification must be submitted to BREC on the appropriate BREC form 2-3 months before the expiry date.

Any amendments to this study, unless urgently required to ensure safety of participants, must be approved by BREC prior to implementation.

Your acceptance of this approval denotes your compliance with South African National Research Ethics Guidelines (2015), South African National Good Clinical Practice Guidelines (2020) (if applicable) and with UKZN BREC ethics requirements as contained in the UKZN BREC Terms of Reference and Standard Operating Procedures, all available at http://research.ukzn.ac.za/Research-Ethics/Biomedical-Research-Ethics.aspx.

BREC is registered with the South African National Health Research Ethics Council (REC-290408-009). BREC has US Office for Human Research Protections (OHRP) Federal-wide Assurance (FWA 678).

The sub-committee's decision will be noted by a full Committee at its next meeting taking place on 10 May 2022.

Yours sincerely,

[redacted]

Prof D Wassenaar
Chair: Biomedical Research Ethics Committee

Biomedical Research Ethics Committee
Chair: Professor D R Wassenaar
UKZN Research Ethics Office Westville Campus, Govan Mbeki Building
Postal Address: Private Bag X54001, Durban 4000
Email: BREC@ukzn.ac.za
Website: http://research.ukzn.ac.za/Research-Ethics/Biomedical-Research-Ethics.aspx

Accepted publications

HIV infection drives interferon signalling within intestinal SARS-CoV-2 target cells

Rabiah Fardoos, Osaretin E. Asowata, **Nicholas Herbert**, Sarah K. Nyquist, Yenzekile Zungu, Alveera Singh, Abigail Ngoepe, Ian Mbano, Farina Karim, Warren Kuhn, Fusi G Madela, Vukani T Manzini, Frank Anderson, Bonnie Berger, Tune H Pers, Alex K. Shalek, Alasdair Leslie and Henrik N. Kløverpris.

JCI Insight. 2021;6(16):e148920. https://doi.org/10.1172/jci. insight.148920.
Contribution: I conducted, analysed and obtained some of the F-IHC images shown in this paper, including all the SARS-CoV-2 nucleoprotein images and created the figure.

Irreversible depletion of intestinal CD4+ T-cells is associated with T-cell activation during chronic HIV infection

Osaretin E Asowata, Alveera Singh, Abigail Ngoepe, **Nicholas Herbert**, Rabiah Fardoos, Kavidha Reddy, Yenzekile Zungu, Faith Nene, Ntombifuthi Mthabela, Dirhona Ramjit, Farina Karim, Katya Govender, Thumbi Ndung'u, J Zachary Porterfield, John H Adamson, Fusi G Madela, Vukani T Manzini, Frank Anderson, Alasdair Leslie, Henrik N Kløverpris.

JCI Insight. 2021 Oct 7:e146162. doi: 10.1172/jci.insight.146162.
Contribution: I conducted, analysed and obtained some of the F-IHC images shown in the paper and edited some images for the resubmission.

Role of Early Life Cytotoxic T Lymphocyte and Natural Killer Cell Immunity in Paediatric HIV Cure/Remission in the Anti-Retroviral Therapy Era

Vinicius A. Vieira, **Nicholas Herbert**, Gabriela Cromhout, Emily Adland, Philip Goulder.

Frontiers in Immunology. 2022 May 11. https://doi.org/10.3389/fimmu.2022.886562.
Contribution: I wrote three chapters, made two figures, and participated in editing this review paper.

Papers in review

Single-cell profiling of environmental enteropathy reveals signatures of epithelial remodeling and immune activation in severe disease

Conner Kummerlowe, Thomas Wallach, Simutanyi Mwakamui, Travis K. Hughes, Nolawit Mulugeta, Victor Mudenda, Ellen Besa, Kanekwa Zyambo, Ira Fleming, Marko Vukovic, Ben A. Doran, Toby P. Aicher, Marc H. Wadsworth II, Juliet Tongue Bramante, Amiko M. Uchida, Rabiah Fardoos, Osaretin E. Asowata, **Nicholas Herbert**, Henrik Kløverpris, John J. Garber, Jose Ordovas-Montanes, Zev Gartner, Alex K. Shalek, Paul Kelly.

Science and Translational Medicine. Resubmitted May 2022.
Contribution: I did histological staining of duodenal and colon pinches (H&E stains, some HIV infected) which were then used for pathological scoring which were used in this paper.